TITLE PAGE

***Classification*:** Biological Sciences, Neuroscience

Title: A Feedback Mechanism Regulates *Odorant Receptor* Expression in the Malaria Mosquito, *Anopheles gambiae*

***Author Line**:* Sarah E. Maguire[a], Ali Afify[a], Loyal A. Goff[a,b], and Christopher J. Potter[a]

Author Affiliation: [a]The Solomon H. Snyder Department of Neuroscience, Johns Hopkins University School of Medicine, Baltimore, MD 21205, USA.

[b]The Department of Genetic Medicine, Johns Hopkins University School of Medicine, Baltimore, MD 21205, USA.

Corresponding author: Christopher J. Potter; Johns Hopkins University School of Medicine, Solomon H. Snyder Department of Neuroscience, Rangos 434, 855 N. Wolfe Street, Baltimore, MD 21205; 443-287-4151; cpotter@jhmi.edu

***Keywords*:** Q-system, olfaction, calcium imaging, single sensillum recordings

ABSTRACT

Mosquitoes locate and approach humans ('host-seek') when specific Olfactory Neurons (ORNs) in the olfactory periphery activate a specific combination of glomeruli in the mosquito Antennal Lobe (AL). We hypothesize that dysregulating proper glomerular activation in the presence of human odor will prevent host-seeking behavior. In experiments aimed at ectopically activating most ORNs in the presence of human odor, we made a surprising finding: ectopic expression of an *AgOr (AgOr2)* in *Anopheles gambiae* ORNs dampens the activity of the expressing neuron. This contrasts studies in *Drosophila melanogaster,* the typical insect model of olfaction, in which ectopic expression of non-native ORs in ORNs confers ectopic neuronal responses without interfering with native olfactory physiology. To gain insight into this dysfunction in mosquitoes, RNA-seq analyses were performed comparing wild-type antennae to those ectopically expressing *AgOr2* in ORNs. Remarkably, almost all *Or* transcripts were significantly downregulated (except for *AgOr2*), and additional experiments suggest that it is AgOR2 protein rather than mRNA that mediates this downregulation. Our study shows that ORNs of *Anopheles* mosquitoes (in contrast to *Drosophila*) employ a currently unexplored regulatory mechanism of OR expression, which may be adaptable as a vector-control strategy.

SIGNIFICANCE STATEMENT

Studies in *Drosophila melanogaster* suggest that insect Olfactory Receptor Neurons (ORNs) do not contain mechanisms by which Odorant Receptors (ORs) regulate OR expression. This has proved useful in studies where ectopic expression of an OR in *Drosophila* ORNs confers responses to the odorants that activate the newly expressed OR. In experiments in *Anopheles gambiae* mosquitoes, we found that ectopic expression of an OR in most *Anopheles* ORNs dampened the activity of the expressing neurons. RNA-seq analyses demonstrated that ectopic OR expression in *Anopheles* ORNs leads to downregulation of endogenous *Or* transcripts. Additional experiments suggest that this downregulation required ectopic expression of a functional OR protein. These findings reveal that *Anopheles* mosquitoes, in contrast to *Drosophila*, contain a feedback mechanism to regulate OR expression. Mosquito ORNs might employ regulatory mechanisms of OR expression previously thought to occur only in non-insect olfactory systems.

Malaria is a major cause of human mortality worldwide (1), and it is a global health imperative to prevent the spread of this disease. Malaria is caused by *Plasmodium* parasites transmitted by the bite of infected *Anopheles* mosquitoes. To date, antimalarial drugs have been the mainstay of control against malaria, and over the past 15 years, these treatments – along with the distribution of insecticide-treated bed nets – have contributed to an overall reduction of disease transmission. However, the eventual eradication of malaria likely rests on a multidisciplinary approach that integrates our knowledge of both host and vector biology (2). For example, impairing the ability of the insect vector to bite a human host may further reduce incidences of infection. As such, disrupting the behaviors that bring mosquitoes to humans could dramatically reduce the prevalence of malaria (3).

Female *Anopheles* mosquitoes locate and approach humans ('host-seek') based on specific cues, such as human-derived odors and exhaled CO_2, moisture and heat emissions, and body shape. The primary way that mosquitoes host-seek is through their sense of smell (olfaction). Mosquitoes have evolved a complex repertoire of chemoreceptors that respond to chemical stimuli such as Ionotropic Receptors (IRs), Gustatory Receptors (GRs), and Odorant Receptors (ORs). Of these, the ORs play a substantial role in mediating how a mosquito responds to human odor (4). ORs form heterotetramer complexes with an obligate co-receptor known as ORCO (5). OR-ORCO complexes are expressed on Olfactory Receptor Neurons (ORNs) of the mosquito's sensory appendages: the antennae, maxillary palps, and labella (6). ORCO-positive ORNs are housed in 'sensilla' or sensory hairs of these appendages. Each sensillum typically contains 1-4 ORNs that each express a unique OR, of which there are 75 in the

Anopheles gambiae genome (7). These ORNs are classified and named by the OR gene they express, and each ORCO-positive ORN class targets a specific brain region of the mosquito Antennal Lobe (AL) known as a glomerulus (8, 9). The decision to approach a human is a direct result of activated ORCO-positive ORNs targeting a *specific* combination of glomeruli (10) (**Fig 1a,b**).

Disrupting this specificity by activating all ORCO-positive ORNs in the presence of human odor has been hypothesized to prevent host-seeking (11, 12). Studies in *Drosophila,* an insect model of olfaction, show that binary systems can be used to express non-native ORs in ORCO-positive ORNs to confer ectopic neuronal responses without interfering with native olfactory physiology. Therefore, we examined whether this strategy could be used to disrupt host-seeking in *Anopheles gambiae* mosquitoes. To test this, we expressed the *Anopheles gambiae odorant receptor 2* (*AgOr2*) in all *Orco*-positive ORNs. AgOR2 is highly attuned to major components of human odor such as benzaldehyde and indole (13), and in the presence of human odor, all *Orco*-positive neurons expressing AgOR2 should become active. Surprisingly, when we evaluated the olfactory physiology of these experimental mosquitoes, we found that they exhibited reduced responses not only to AgOR2's cognate ligands (benzaldehyde and indole) but to odors in general. To investigate the molecular basis of this phenotype we looked for signatures of disfunction at the level of the transcriptome. Using RNA-seq to compare transcript levels from wild-type antennae to those ectopically expressing *AgOr2,* we discovered that *odorant receptor* isoforms were significantly downregulated in the experimental line while the remaining transcripts were largely unchanged. Additional experiments revealed that it is AgOR2 protein rather than *AgOr2 mRNA* that reduces

native *odorant receptors* levels. Overall, our study suggests the existence of a feedback mechanism of *odorant receptor* regulation whereby an OR protein downregulates the transcripts of alternative *Or* genes.

RESULTS

Ectopically Expressing *AgOr2* in *Orco*-positive Neurons Impairs Olfactory Physiology. To activate *Orco*-positive ORNs in the presence of human odor, we used 'olfactogenetics,' a technique whereby a specific volatile odorant is used to activate a defined set of OR-expressing neurons (14). To accomplish this, an *Or* with known response properties is ectopically expressed in ORNs of interest through the use of a binary expression system, such as the Q-system (15) or the *UAS*-Gal4 system. Thus, in the presence of odors in which the introduced OR normally responds, olfactory receptor neurons with ectopic expression become active.

In 2016, the Q-system was introduced into *Anopheles,* making it possible to adapt olfactogenetics in mosquitoes (6). As a binary expression system, the Q-system works by directing the expression of a specific gene into a specific cell population. This particular system relies on two elements: QF2 and *QUAS*. The QF2 transcription factor is expressed under the control of a cell-type specific enhancer/promoter and binds to its upstream activating sequence, *QUAS*. Once bound by QF2, *QUAS* initiates transcription of its effector gene. To ectopically activate *Orco*-positive ORNs in the presence of human odor, we combined a mosquito line containing *Orco-QF2* (6), which contains a fusion between the presumptive enhancer and promoter regions of the gene

Orco and the transcription factor QF2, with an effector line containing a *QUAS* transgene upstream of the *Anopheles gambiae odorant receptor 2, AgOr2 (QUAS-AgOr2)*. Thus, experimental animals exhibit ectopic expression of *AgOr2* in all *Orco*-positive ORNs (**Fig. 1c**).

AgOR2 is highly attuned to major components of human odor such as benzaldehyde and indole (16) and it was expected that *Orco*-positive ORNs of *Orco>AgOr2* mosquitoes would become active in the presence of these cognate ligands, essentially activating the majority of the olfactory system during host-seeking (**Fig. 1d**). To test the functional activity of olfactory receptor neurons ectopically expressing *AgOr2* in mosquitoes, we imaged the calcium response of *Orco>AgOr2* antennal segments in a *QUAS-GCaMP6f* background (*Orco>AgOr2,GCaMP6f)*. Surprisingly, *Orco>AgOr2,GCaMP6f* antennae showed a dampened response not only to various concentrations of benzaldehyde and indole, but to odors in general (**Fig. 2a**). For example, octenol potentially activates 31 different *Anopheles gambiae* ORs (16), but the olfactory receptor neurons of the experimental mosquitoes did not show a response to this odor. In *Drosophila*, a single ORN class can drive behavior at spike rates as low as 10-20Hz (10). When we stimulated *Orco>AgOr2,GCaMP6f* with 5 additional odors known to activate 14-16 different ORN classes at rates higher than 50 spikes/sec (16), the olfactory receptor neurons still did not exhibit odor-induced responses (**Fig. S1**).

One possibility for the observed olfactory defects (**Fig. 2a, Fig. S1**) is that the *QUAS-AgOr2* transgene inserted into an endogenous olfactory gene and disrupted olfactory functions. As determined by splinkerette mapping (17), the insertion site of the

QUAS-AgOr2 line examined in **Fig. 2a and Fig. S1** (line 1) is located in an intergenic region on chromosome 3R between the genes ACOM029303 and ACOM029196. While it is unlikely that this particular insertion site would disrupt the function of an olfactory gene necessary for ORN physiology, we extended our studies to analyze the physiology of two additional *QUAS-AgOr2* lines inserted into different regions of the genome. We established line *QUAS-AgOR2#2*, which maps to an intergenic region between ACOM036217 and ACOM036230, and line *QUAS-AgOR2#*3, which could not be mapped by splinkerette PCR. When driven into *Orco*-positive cells, all three lines show similar defects in olfactory physiology when compared to wild-type (**Fig. S2**). Furthermore, since these lines were tested as heterozygotes, any recessive mutation in an olfactory gene caused by the *QUAS-AgOr2* insertion should be compensated by the wild-type allele. Overall, these data show that the dominant negative olfactory phenotype (**Fig. 2a, Fig. S1, Fig. S2**) is a consequence of ectopic *AgOr2* expression rather than the genomic insertion site of the *QUAS-AgOr2* element.

Olfactogenetics Impairs *Anopheles* but not *Drosophila Orco*-positive ORNs. Ectopically expressing an *Or* in *Drosophila* ORNs causes the expressing neuron to activate in the presence of the introduced OR's odor ligand (14, 16, 18-20). One possibility as to why *Orco>AgOr2* cells in the mosquito did not respond to benzaldehyde or indole was because the *AgOr2* sequence used to create the transgenic *QUAS-AgOr2* line was perhaps acting in a dominant-negative manner to disrupt ORCO/OR_X ion channels. To test this, we ectopically expressed *AgOr2* in *Drosophila Orco*-positive neurons using the GAL4-UAS system and measured the response rate of neurons

168 housed in the ab1 sensilla using Single Sensillum Recordings (SSR). Ab1 contains 4
169 olfactory neurons: 3 of which are *Orco*-positive and express *Or10a*, *Or42b*, and *Or92a*,
170 and one of which is *Orco*-negative and expresses the gustatory receptor *Gr21*, which
171 responds to CO_2. To determine whether ectopic expression of *AgOr2* impairs native OR
172 responses to their cognate ligands, responses of the OR10a-expressing neuron to
173 methyl salicylate were measured. We found no difference in how control (*Orco-GAL4)*
174 and experimental *(Orco>5xAgOr2)* sensilla responded to methyl salicylate, indicating
175 that *AgOr2* expression does not interfere with the olfactory physiology of the neuron in
176 which it is expressed. Furthermore, native responses of OR10a were not affected when
177 an even higher dosage of *AgOr2* was driven into the neuron (*Orco>20xAgOr2)* (**Fig.**
178 **2b**). When we puffed benzaldehyde over the experimental preparation, *Orco*-positive
179 cells in the *Drosophila* ab1 sensilla ectopically respond. Interestingly, sensilla that have
180 higher levels of ectopic *AgOr2* can still maintain ectopic responses without
181 compromising neuron function. When we used the stronger effector line (*20XUAS)* to
182 ectopically express *AgOr2* in *Drosophila Orco*-positive neurons, the olfactogenetics
183 approach continued to work and olfactory physiology was not impaired.

184 The *Anopheles* capitate peg (cp) sensillum is similar to the ab1 sensillum of
185 *Drosophila* as it contains *Orco*-positive ORNs, which express *Or8* and *Or28,* and one
186 *Orco*-independent olfactory neuron that responds to CO_2. When we ectopically
187 expressed *AgOr2* in *Orco*-positive ORNs in the mosquito and recorded from cp sensilla,
188 we found that the OR8-expressing neuron's response to octenol, its cognate ligand, was
189 eliminated (**Fig. 2c**). In addition, neither OR8 nor OR28-expressing neurons ectopically
190 respond to benzaldehyde. Similar to *Drosophila*, the genetic manipulation does not

affect the physiology of the *Orco*-negative CO_2-responsive neuron (**Fig**. **2c**). These data indicate that olfactogenetics affects the physiology of *Drosophila* and *Anopheles Orco*-positive ORNs differently: in flies, ectopically expressing *Or*s does not affect endogenous neuronal function, whereas in *Anopheles* mosquitoes, ectopic expression of an *Or* disrupts the function of the olfactory receptor neurons.

Ectopic AgOR2 protein eliminates olfactory responses in *Orco*-positive cells. It is possible that driving an *Or* into an *Anopheles* ORN is cytotoxic, especially if the neuron experienced continual stimulation from the environment. To assess whether this was the case, we examined the anatomy of the AL and ORN projections in *Orco>AgOr2* mosquitoes, to check for intact neuronal processes. As shown previously (6), ablating *Orco*-positive cells would cause their ORN projections to be eliminated in the AL. Using immunochemistry to visualize ORN terminals in the AL, both the ORN projections and the AL in general remained intact, indicating that the lack of ORN responses to odor was not due to the death and elimination of neurons ectopically expressing *AgOr2* (**Fig. S3**). Next we tested if driving any generic transmembrane protein into *Anopheles* ORNs also hindered olfactory physiology. To evaluate this, we used the *Orco-QF2* driver to ectopically express the transmembrane protein *mCD8::GFP* (6) into all *Orco*-positive neurons. There were no differences in the odor-induced responses between control and *mCD8::GFP*-positive ORNs (**Fig. S4**), suggesting that ectopic expression of another transmembrane protein did not silence ORN activities.

Ectopic *AgOr2* expression may inhibit olfactory responses either at the level of the *AgOr2* RNA or at the level of AgOR2 protein. To distinguish between these two

possibilities, we created a transgenic mosquito line containing a mutated version of *AgOr2 (mutAgOr2)* that contained a mutation in the start codon of *AgOr2* such that *QUAS-mutAgOr2* produced mRNA that cannot be translated when combined with *Orco-QF2*. We also induced a frameshift mutation at a second in-frame ATG site in *mutAgOr2* to eliminate the possibility of having an alternative open reading frame used during translation. We crossed *QUAS-mutAgOr2* with *Orco-QF2,QUAS-GCaMP6f* and found that the calcium responses were not compromised (**Fig. 3**); only when the functional version of the protein was expressed (*QUAS-AgOr2*) was the odor response impaired (**Fig. 2a,c, Fig. S1, Fig. S2**). Taken together, these data indicate that AgOR2 protein itself, and not mRNA, was largely responsible for the olfactory defect of *Orco*-positive cells.

Ectopic AgOR2 Reduces the Transcripts of Native *Ors.* How might AgOR2 protein impair olfactory responses? We hypothesized this may occur as a result of 1) regulatory mechanisms affecting *Or* transcription, stability, and/or degradation rates or 2) regulatory mechanisms and/or defects in OR protein function. These transcriptional or post-translational mechanisms may act together, or independently. To distinguish between these two possibilities, we performed isoform-level RNA-seq on antennae isolated from control and *Orco>AgOr2* samples. Of the ~13,000 transcript isoforms detected, only 83 were differentially expressed in the *Orco>AgOr2* mosquito antennae. Interestingly, half of these differentially expressed isoforms (41/83) were *Ors*, which were all downregulated in *Orco>AgOr2* antennae, except for *AgOr2*, which was highly upregulated (**Fig. 4a**). As shown by the *Or* isoform comparison heatmaps in **Figure 4b**,

control *Or* levels are higher than those in *Orco>AgOr2,* with the exception of *AgOr2*, which is upregulated.

If AgOR2 ectopic protein was responsible for modulating the steady state abundance of native *Or* transcripts, then the relative abundance of the *odorant receptor* gene family isoforms in *Orco>mutAgOr2* antennae should not be affected. To test this, we extracted biological triplicates of mosquito antennae from female mosquitoes of the *Orco>mutAgOr2* line and compared the isoform abundance levels of this group to the original RNA-seq dataset. Ternary plots depicting the relative abundance of isoform expression levels in control, *Orco>mutAgOr2*, and *Orco>AgOr2* conditions as a position on an equilateral triangle were used to explore how *Or* and other gene sets were differentially expressed. To depict how control, *Orco>mutAgOr2*, and *Orco>AgOr2* contribute to relative isoform abundances of non-*Or* genes and *Or* genes, we created 2 discrete ternary plots. As expected, the relative contribution of control, *Orco>mutAgOr2*, and *Orco>AgOr2* for all non-*odorant receptor* isoform in the transcriptome was roughly equal (34.3%:33%:32.6%). However, when removing the contribution of the ectopically induced *AgOr2* from the *Or* isoform pool, the ratio for the *odorant receptor* family was skewed to 45.8%:37.8%:16.4% (control:*Orco>mutAgOr2*:*Orco>AgOr2*) (**Fig. 4c**), indicating that the relative contribution of an *Or's* abundance level was roughly equal among control and *Orco>mutAgOr2* groups, but reduced in *Orco>AgOr2*. Results of the gene set enrichment test and pairwise comparisons of *Or* isoforms can be viewed in **Figure S5**. The majority of native *Ors* are downregulated in *Orco>AgOr2* but not in *Orco>mutAgOr2,* with four exceptions: *Or2, Or16, Or17,* and *Or33*.

As visualized by the onset of ORCO expression, ectopic AgOR2 is driven immediately after larval-pupal ecdysis. We next examined when, during the life cycle of the mosquito, the downregulation of native *Or* genes via ectopic AgOR2 expression might occur. Since ectopic AgOR2 expression is dictated by the *Orco* enhancer/promoter region (**Fig. 1c**) (6), AgOR2-induced olfactory silencing of native *Or* genes should coincide with the ORCO expression pattern. Mosquitoes experience four different developmental stages during their lifespan: egg, larvae, pupae, and adult stages. During the pupal stage, adult features of the mosquito olfactory system take shape (21, 22), so we examined this stage of development for the onset of ORCO expression. To document this, we extracted and stained pupal antennae from *Orco>mCD8::GFP* mosquitoes every 4hrs starting at the onset of pupal development (After Puparium Formation: 0-2hr APF) to just before eclosion (20-22hr APF), which happens at 24hrs APF. ORCO (as reported by mCD8) was expressed immediately after pupal ecdysis, just 0-2hrs APF (**Fig. S6a**). Interestingly, ORCO expression turns on gradually in the developing antennal ORNs, where each flagellomere gains ~15 Orco-positive cells every 4hrs, starting from ~8 cells at 0-2hr APF and ending with ~87 cells per flagellomere at 4hrs before eclosion (**Fig. S6b**). These data suggest that ectopic expression of AgOR2 (which should coincide with ORCO) also occurs throughout pupal development, and might impinge upon developmental mechanisms that regulate *Or* expression. The timepoint at which native *Or* genes begin to express in *Anopheles* is not currently known, but in *Aedes aegypti* several *Ors* (in addition to *Orco*, as detected by *in situs*) are present 3/4ths of the way through the pupal stage (23). This suggests that in natural conditions, negative inhibition of *AgOr* genes by AgOR protein might

283 occur during the pupal stage, when adult features of the olfactory system are being
284 developed.
285
286 **Impairing *Orco*-positive neuron responses does not inhibit host-seeking behavior**
287 **in *Anopheles* mosquitoes.** In the absence of an *Orco* mutant, the olfactory phenotype
288 of *Orco>AgOr2* mosquitoes presented the opportunity to test whether *Anopheles*
289 mosquitoes without ORN function still host-seek. DeGennaro et al. 2013 (4) found that a
290 null mutation of the *Orco* gene in *Aedes* mosquitoes did not prevent host-seeking
291 behavior (presumably due to redundant function of IR neurons (24)), but whether the
292 malaria mosquito would behave similarly is unknown. To test whether *Orco>AgOr2*
293 mosquitoes showed reduced attraction towards human hosts, we used the 'host-
294 proximity assay' (4), a population assay that measures the proportion of females that
295 come into olfactory (but not physical) contact with a human arm. As found with *Orco*
296 mutant *Aedes* mosquitoes (4), *Anopheles* mosquitoes without functional *Orco*-positive
297 neurons were still attracted to a human host (**Fig. 5a-c).**
298
299 **DISCUSSION**
300
301 We report for the first time, to our knowledge, an unexplored mechanism of *Or*
302 regulation in *Anopheles* mosquitoes that diverges from the dogma established in
303 *Drosophila*. A main finding of our paper – that OR protein downregulates the expression
304 of native *Ors* (**Fig. 5d**) – is a pattern more closely resembling OR-regulatory processes
305 in mice than those of *Drosophila.* As this (**Fig. 2b**) and previous studies have

306 demonstrated (14, 18, 20) driving ectopic expression of an *Or* in non-native *Orco*-
307 positive ORNs does not disrupt *Drosophila* neuron function whereas in *Anopheles* it
308 does (**Fig. 2a,c, Fig. S1, Fig. S2**). Furthermore, ectopically expressing an *Or* gene in
309 *Drosophila* ORNs does not affect gene expression of native *Ors* (20), whereas a similar
310 manipulation in *Anopheles* leads to robust changes in gene expression (**Fig. 4**).

311 From these experiments, we hypothesize unexpected similarities of *Or* gene
312 regulation between *Anopheles* and mice. For example, both *Anopheles* and mice
313 contain a negative feedback loop by which OR protein inhibits the expression of
314 alternative *Ors*. In *Anopheles* mosquitoes (**Fig. 3, Fig. 4**) as was the case in mice, this
315 feedback pathway requires intact OR protein (with 3 exceptions: see **Fig. S5**) since
316 expressing mutant *Or* genes lacking either the entire coding sequence or the start
317 codon permits a second *Or* gene to be expressed (25-28). Frameshift mutations also
318 allow for the co-expression of functional *Or* genes (25). It remains to be determined if
319 this repression in *Anopheles* olfactory receptor neurons utilizes similar cellular
320 machinery as in mice (29).

321 What might be the selective advantage of an *Anopheles* mosquito *Or* feedback
322 mechanism? One possibility is that it increases the likelihood that a single olfactory
323 receptor neuron expresses only 1 OR. This is an important developmental mechanism
324 in mice, where ORs play an instructive role in guiding olfactory receptor neuron axonal
325 projections to the olfactory region of the brain (30-32). In analogous experiments to
326 those presented here, when multiple ORs are genetically engineered to co-express in a
327 single olfactory receptor neuron in mice, the topographic map of projections to the
328 olfactory center in the brain is perturbed (33). While we do not know when native *Or*

329 genes turn on or when ORNs target the AL in *Anopheles*, our methods expressed
330 *AgOr2* in *Orco* neurons as early as 0-2hr APF (**Fig. S6**). If ORNs have not yet targeted
331 the AL at this early stage, our data suggests that *Ors* in mosquitoes are likely not
332 involved in axon guidance, as we did not detect major deformations of ORN targeting or
333 AL structure in the adult brain (**Fig. S3**). What might be another biological process
334 influenced by OR gene regulation? If this mechanism functions during adulthood, it
335 could be important for synchronizing a mosquito's dynamic biological needs in the
336 environment with the physiology of olfactory receptor neurons. Mosquitoes rely heavily
337 on their sense of olfaction to integrate ecologically relevant stimuli that change over the
338 course of their adult lifespan. When females first eclose, they are uninterested in host
339 odor (34) and instead actively search for sugar-rich resources from plants to
340 supplement their nutrient reserves. After a period of ~4 days post eclosion, they develop
341 an attraction to host odors (34, 35) and following a bloodmeal will experience a
342 refractory period to host odor until after oviposition. These changes in behavior have
343 been correlated with changes in chemosensory gene transcript abundance (34, 36). It
344 would be interesting to determine if expression of alternative *Ors* in ORNs only during
345 adulthood – when endogenous ORs are already chosen – can alter *Or* gene expression,
346 or if precocious expression of *Ors* takes on an 'early-bird-gets-the-worm' paradigm (37).
347 *AgOrs* can be co-expressed within the same ORN when transcribed as
348 polycistronic mRNA (38). Polycistronic *Or* mRNA is observed in cases when *Or* genes
349 are clustered tightly together within the genome. Such clustering of *Or* genes is
350 commonplace in mosquito species such as *Anopheles gambiae* (39) and *Aedes aegypti*
351 (40), as well as in mice (41, 42); however, to our knowledge, polycistronic *Or* mRNA has

not been observed in rodent olfactory systems. It is possible that polycistronic *Or* expression avoids the negative feedback mechanism of *Or* regulation, enabling the neuron to co-express multiple *Ors*.

While ectopically expressing *AgOr2* downregulates native *Or* genes, it was surprising that *Orco>AgOr2* neurons did not show responses to the cognate ligands of AgOR2 (benzaldehyde and indole). Our RNA-seq data indicates that while native *Or* transcripts are reduced, *AgOr2* transcripts are 3x higher than in wild-type conditions: if *AgOr2* transcripts are being translated, this could lead to 3x the amount of AgOR2 protein. We hypothesize that elevated AgOR2 protein levels may be disrupting the stoichiometry of the AgOR2-ORCO complexes, rendering them non-functional. While research has shown that ORs form stable heteromeric complexes with ORCO (43-46), the stoichiometry underlying OR-ORCO channels is unknown. RNA-seq data from this study and from two independent studies show that in wild-type conditions, there is a conserved ~1:1 relationship between *Orco* and total *Or* transcripts (47, 48). Interestingly, we see that ectopic *AgOr2* expression does not change *Orco* expression (**Fig. 4b**), skewing the ratio in experimental conditions to 1:3. We predict this skewed OR expression in a neuron causes major disruptions at the level of the AgOR2:ORCO protein complex. This may result in a trafficking defect in which AgOR2:ORCO complexes do not migrate to the cell surface. Since Orco is required to traffic OR:ORCO complexes to the dendritic surfaces (43), increasing AgOR2 expression might interfere with this process. Alternatively, changes to the OR:ORCO stoichiometry might result in a functional defect in the channel itself, whereby the malformed complexes cannot respond to odors even if they have been successfully trafficked to the membrane.

375 This study adds to the mounting evidence that the disruption of a single sensory
376 modality is insufficient to completely eliminate host-seeking behavior in mosquitoes. As
377 first demonstrated in *Aedes aegypti,* mosquitoes with a mutation in the *Orco* gene
378 remain attracted to humans (4); similarly, we find that *Anopheles* mosquitoes with
379 impaired ORCO neuronal function continue to host-seek (**Fig. 5a-c**). In addition to
380 odors, mosquitos are attracted to a wide variety of human-derived cues, including heat,
381 CO_2, visual stimuli, and moisture; and so one sensory modality is likely able to
382 compensate for the loss of another (4, 24, 49, 50).

383 Our study uncovers the existence of a mechanism of *Or* regulation in insects
384 whereby expression of an OR protein results in the downregulation of other native *Or*
385 gene isoforms (**Fig. 5d**). This work lays the foundation to explore specific cellular
386 mechanisms utilized by mosquito olfactory receptor neurons to regulate *Or* expression.
387 A mechanism of OR regulation in mosquitoes may also be a target for vector-control
388 strategies to alleviate the spread of vector-borne diseases.

389

390 **METHODS**

391 **Insect stocks.** *Mosquitoes. Orco-QF2* and *QUAS-mCD8::GFP* transgenic mosquito
392 stocks were generated as described in Riabinina et al. 2016 (6). *QUAS-GCaMP6f* was
393 generated as described in Afify et al. 2019 (51). Wild-type Ngousso mosquitoes were a
394 gift from the Insect Transformation Facility (Rockville, MD). *Flies. Orco-GAL4* (#26818)
395 and *5xUAS-AgOr2* (#58828) lines were obtained from the Bloomington *Drosophila*
396 Stock Center.

Recombinant DNA construction. Plasmids were constructed by enzyme digestions, PCR, subcloning and the In-Fusion HD Cloning System (Clontech, catalogue number 639645). Plasmid inserts were verified by restriction enzyme digests and DNA sequencing. Insertions of each plasmid into the *Anopheles* genome (*QUAS-AgOr2, QUAS-mutAgOr2*) or the *Drosophila* genome (*20xUAS-AgOr2*) were verified by sequencing the vector-specific cassette within the transgenic animal.

To create the *pXL-BacII-15xQUAS-TATA-AgOr2-Sv40* reporter line, we linearized the *pXL-BacII-15xQUAS_TATA-Sv40* (6) vector with *XhoI*. The cDNA of *AgOr2* was amplified from Bloomington stock number 58828 using the oligos *Aga_OR2_F* (5'-ATTCGTTAACAGATCTATGCTGATCGAAGAGTGTCCGA-3') and *Aga_OR2_R* (5'- CCTTCACAAAGATCGACGTCTTAGTTGTACACTCGGCGCAGC-3'). The resultant PCR product was then infusion-subcloned back into the construct. To create the *pXL-BacII-15xQUAS-TATA-mutAgOr2-Sv40* reporter line, we did a double digest of *pXL-BacII-15xQUAS-TATA-AgOr2-Sv40* with *BglII* and *XhoI*. We then amplified *AgOr2* from *pXL-BacII-15xQUAS-TATA-AgOr2-Sv40* using a forward primer that mutated the start codon: ATG→TTT (*InfuMUTAgOr2_for*: 5'-ATTCGTTAACAGATCTTTTCTGATCGAAGAGTGTCCGATAATTG). We also engineered the reverse primer to create a frameshift mutation at a second in-frame ATG site located between the first and second transmembrane domains of *AgOr2* (*InfuMUTAGOr2_rev*: 5'- CGTCATTTTTCTCGAGTAGAGAGCGTACTCGGCGGC-3').

The *20xUAS-AgOr2* reporter was created in *Drosophila* to test whether increasing the dosage of *AgOr2* affects olfactory physiology. The construct was made by digesting *pJFRC-20xUAS-IVS-CD8GFP* with *NotI* and *XbaI* and isolating the

linearized 8.1kb vector. *AgOr2* was PCR amplified from *pXL-BacII-15xQUAS-TATA-AgOr2-Sv40* using the primers *UAS-AgOr2-FOR* (5'-TTACTTCAGGCGGCC GCAAA ATGCTGATCGAAGAGTGTCCG) and *UAS-AgOR2-REV* (5'-ACAAAGATCCTCTAGA TTAGTTGTACACTCGGCGCAG-3'). The PCR product was infusion cloned into the digested *pJRFRC-20xQUAS* vector. Upon sequence confirmation, the plasmid was midiprepped (Qiagen 12145) and sent to Rainbow Transgenics for injection into the attP site (RFT # 8622).

The *pXL-BACII-DsRed-OR7_9kbProm-QF2-hsp70* construct was used by the *Orco-QF2* driver line in this study. Construction of this plasmid is described in Riabinina et al. 2016 (6).

***Anopheles gambiae* transgenics.** *Anopheles gambiae* M-form strain Ngousso (the M-form of *An. gambiae* is now referred to as *Anopheles coluzzii*) mosquitoes were grown at 28°C, 70-75% relative humidity, 12h light/dark cycle. Freshly deposited eggs were collected by providing mated, gravid females with wet filter paper as an oviposition substrate for 15-20min, after which the eggs were collected and systematically arranged side-by-side on a double-sided tape fixed to a coverslip. Aligned embryos were covered with halocarbon oil (Sigma, series 27) and injected at their posterior pole with an injection cocktail between 30-40min after egg laying. Injection cocktails consisted of a mixture of two plasmids, one with a piggyBac vector carrying the transgene of interest with a dominant visible marker gene – enhanced cyan fluorescent protein (ECFP) – under the regulatory control of the *3xP3* promoter, and a piggyBac transposase-expressing plasmid consisting of the transposase open reading frame under the

443 regulatory control of the promoter from the *An. stephensi vasa* gene. Vector
444 concentrations were at 150ng/uL and the transposase-expressing plasmid was at
445 300ng/uL in 5mM KCL, 0.1mM sodium phosphate pH 6.8. Halocarbon oil was
446 immediately removed and coverslips with injected embryos were placed in trays of
447 water at 28°C, where the first instar larvae hatched ~24hr later. The Insect
448 Transformation Facility (https://www.ibbr.umd.edu/facilities/itf) within the University of
449 Maryland College Park's Institute for Bioscience and Biotechnology Research
450 performed all embryo microinjections. Adults developing from injected embryos were
451 separated by sex at the pupal stage before mating, and small groups of 5-10 injected
452 adult males or females were crossed to wild-type Ngousso adults of the opposite sex.
453 The progeny from these matings were screened during the third or fourth larval instar
454 for the presence of vector-specific marker gene expression. Transgenic larvae were
455 saved and adults from these larvae were outcrossed to wild-type for a total of 5
456 generations.
457
458 **Insect stock maintenance.** *Anopheles gambiae. Anopheles* mosquitoes were grown at
459 28°C, 70-75% relative humidity and 14hrlight/10hr dark cycle. Larvae were reared at low
460 densities (175 larvae/1L dH_2O) to ensure large adult size. They were provided with
461 TetraMin Tropical Flakes and Purina Cat Chow Indoor pellets *ad libitum*. Pupae were
462 hand collected and allowed to eclose in small cages, where they were provided with
463 10% sucrose continuously. Almost all pupae eclosed the day after collection. Adult
464 males and females were kept together in the same cage for 7-10 days, after which they
465 were fed mouse blood from anaesthetized mice according to Johns Hopkins University

Animal Care and Use Committee (ACUC) approved protocol #M019M483. Eggs were collected from the resulting gravid females by providing them with a cup of water containing wet filter paper on which to deposit their eggs as an oviposition substrate. Each generation was screened for the presence of the eye specific marker encoded by the inserted plasmid cassette. *Drosophila melanogaster.* Flies were reared at 25°C and 70% humidity on a standard cornmeal diet.

Calcium imaging. *Preparation. In vivo* preparation of mosquitoes (ages 3-10 days) and optical imaging of odor-evoked calcium responses are described in Afify et al. 2019 (51). *Genotyping mosquitoes.* After the recordings were made for each sample, we froze the bodies of all mosquitoes for subsequent gDNA extraction and genotyping. At the time of the experiment, our transgenic lines were not homozygous. Because all *QUAS* effector lines (*QUAS-AgOr2, QUAS-mutAgOr2*, *QUAS-GCaMP6f*) are marked with the dominant eye marker, ECFP, we had to determine – for each sample – whether the mosquito contained a single copy of *QUAS-AgOr2*, a single copy of *QUAS-GCaMP6f*, or both *QUAS-AgOr2* and *QUAS-GCaMP6f* transgenes (for experiments in **Fig. 2 and S1-2**). For the experiment in **Fig. 3**, we had to determine – for each sample – whether the mosquito contained a single copy of *QUAS-mutAgOr2*, a single copy of *QUAS-GCaMP6f*, or both *QUAS-mutAgOr2* and *QUAS-GCaMP6f* transgenes. To genotype *QUAS-GCaMP6f*, we used the primers *gcamp6f_for2* (5'-ATGGTATGGCTAGCATGACTG-3') and *gcamp6f_rev* (5'-GTAGTTTACCTGACCATCCCC-3'). Females that did not have any amplification of *GCaMP6f* were discarded from the analysis. To genotype *QUAS-AgOr2* or *QUAS-*

mutAgOr2, we used the following primers: *AgOr2_for1* (5'-TAATTGGTGTCAATGTGCGAG-3') and *AgOr2_rev2* (5'-TTATCGGCTCCTCAAAGTCTG-3'). The PCR was designed so that both the wild-type *AgOr2* (1542bp) and the transgenic *AgOr2* (966bp) (or *mutAgOr2;* 968bp) – if present – would amplify. For each female, we determined whether she contained the wild-type and transgenic copy of *AgOr2* (or *mutAgOr2*) or only the wild-type *AgOr2*. Scoring of all calcium imaging files was done blind to genotype. *Analysis.* To make the heatmaps (ΔF), Fiji software (52) was used with a custom-built macro. This Macro uses the "Image stabilizer" plug-in to correct for movements in the recording, followed by the "Z project" function to calculate the mean baseline fluorescence (mean intensity in the first 9s of recording, before stimulus delivery). The "Image calculator" function was used to subtract the mean baseline fluorescence from the image of maximum fluorescence after odorant delivery (this image was manually chosen). Afterward, this ΔF image was used to produce heatmaps. To quantify the ΔF value for each segment to each odor, the "ROI manager" tool in Fiji was used to manually select an ROI. For each sample, we manually drew the 'antennal ROI' around the 11th antennal segment from an epifluorescent image taken for each sample prior to the calcium imaging. We also drew a 'background ROI' outside of the tissue using the same surface area as the 'antennal ROI' to control for any background signal. A "task manager" was used to store the location of the antennal ROI and the background, and the mean intensity across the antennal segment (or background control) for each odor was stored for each ROI. The final ΔF value was taken for each antennal segment and each odor as the mean intensity of the 'antennal ROI' minus the 'background ROI.' Of note, the imaging

512 software was upgraded for **Fig. 3**, which explains why the (ΔF) values in **Fig. 3** are on a
513 different scale than **Fig. 2, Fig S1**, and **Fig. S2**. Data were analyzed using JMP Version
514 9, SAS Institute Inc., Cary, NC, 1989-2019.
515
516 **Single Sensillum Recordings (SSR)**. *Drosophila preparation.* Flies were housed on
517 regular food in groups of a maximum of 10. Analysis was done on ab1 sensilla from 6-
518 10 day old male flies. Sensilla of targeted ORNs were prepared and identified using
519 methods described in Lin & Potter 2015 (53). Briefly, ab1 sensilla were identified by
520 their response to CO_2. Ab1 is the only sensillar group that houses the CO_2-responsive
521 neuron, and so a CO_2-response was indicative that the sensillum we were recording
522 from was ab1. Signals were amplified 100X (USB-IDAC System; Syntech, Hilversum,
523 The Netherlands), inputted into a computer via a 16-bit analog-digital converter and
524 analyzed off-line with AUTOSPIKE software (USB-IDAC System; Syntech). The low
525 cutoff filter setting was 50Hz, and the high cutoff was 5kHz. To deliver odors or CO_2 to
526 ab1, a constant air stream was guided through a serological pipette with a tip placed
527 1cm from the antennae. The chemical cartridge was laterally inserted into this airflow.
528 Stimuli consisted of 1000ms air pulses passed over odorant sources, which were
529 various odorants diluted in paraffin oil (30μL on a filter paper of 1x2cm). For the
530 benzaldehyde analysis, we counted every spike (did not distinguish among neuron
531 subtypes). For the methyl salicylate analysis, we only included the response from the
532 DmOR10a-positive neuron. Delta spikes/second were calculated by manually counting
533 the number of spikes in a 0.5s window at stimulus delivery (200ms after stimulus onset
534 to account for the delay due to the air path) and then subtracting the number of

spontaneous spikes in a 0.5s window before stimulation, multiplied by 2 to obtain delta spikes per second. *Mosquito preparation.* Mated females were 5-12 days old and not bloodfed. Extracellular recordings of the capitate pegs on the maxillary palps were made using the same equipment as for *Drosophila* SSR (see above). Cp sensilla were also identified by their response to CO_2. Cp is the only sensillum that houses the CO_2-responsive neuron, and so a CO_2-response was indicative that the sensillum we were recording from was cp. SSR data were analyzed using JMP Version 9, SAS Institute Inc., Cary, NC, 1989-2019.

RNA-seq. To generate experimental pools of *Orco>AgOr2* antennae, mosquitoes of the genotype *QUAS-AgOr2* were crossed to *Orco-QF2*. Simultaneously, we generated control samples by crossing our *Orco>AgOr2* or *Orco-QF2* strains to wild-type (2 crosses). All 3 crosses were conducted in large breeding cages that consisted of ~75 males and ~75 females. Crosses were blood-fed a total of 4 times and progeny from each cross were screened for the eye-specific fluorescent markers. Larvae generated from experimental crosses were screened for the presence of ECFP and DsRed, markers for the *QUAS* and the *Orco-QF2* transgenes, respectively. Larvae that did not contain both markers were discarded. For the control larvae progeny, animals that contained a single eye marker (either DsRed or ECFP, respectively) were kept in control pools that consisted either of *Orco-QF2* or *QUAS-AgOr2* alone. All mosquitoes used in this study were heterozygous for a given transgene. *Orco>mutAgOr2* and *QUAS-mutAgOr2* library preparations were made using the procedure described above with the exception that the antennae were extracted at a different time. To prepare

antennal RNA-seq libraries, we isolated RNA from approximately 200 antennae from age-matched cohorts (11 total samples: 3 experimental samples containing *Orco>AgOr2* antennae (*orco-QF2* + *QUAS-AgOr2*), 5 control samples consisting of 2 samples from *Orco-QF2* antennae, 2 samples from *QUAS-AgOr2* antennae, and 1 sample from *QUAS-mutAgOr2* antennae, and 3 experimental samples containing *Orco>mutAgOr2* antennae). These mated females were within their fertile period (5-20 days old) and did not receive a bloodmeal.

To create the antennal RNA-seq libraries, we removed the whole antennae from the base of the pedicel and isolated total RNA using TriZol purification methods. The tissues were disrupted and homogenized using a power pestle with disposable RNAse free pestles. Total RNA samples were stored at -80°C and shipped to Genewiz Inc, where they were first assessed for quantity (Qubit Quantification) and quality (Agilent 2100 Bioanalyzer). RNA library preparation with polyA selection was then carried out using the *Illumina* HiSeq with a 2x150bp configuration. Paired end reads were pseudoaligned to the AgamP4.12 reference transcriptome (7) and isoform-level abundances were quantified using kallisto v0.46.0 (54) using default parameters with the following exceptions: `-t4 and -b100`. Per-sample abundances were aggregated and normalized in R using sleuth v0.30.0 (55). For each pairwise comparison (AgOr2 v control, mutAgOr2 v control, and mutAgOr2 v AgOr2), we fit a full sleuth model using condition as an explanatory variable. Differentially expressed isoforms were identified using the Wald test ($q \leq 0.01$, Benjamini-Hochberg corrected) for each model fit. Ternary plots were constructed using the ggtern R package (56).

The RNA-seq raw reads and dataset analyses are available from NCBI. The accession numbers are: (TBD)

Immunohistochemistry *Brains.* Brains of female mosquitoes of *Orco>mCD8::GFP* and *Orco>AgOr2,mCD8::GFP* genotypes were extracted and stained as described previously (6). Once genotyped via a PCR designed to amplify the transgenic and wild-type copies of *AgOr2* (see 'Calcium imaging section' above), experimental and control brains were separated and stained in two different groups. Rat anti-CD8 (Invitrogen #MCD0800, 1:100) was used to visualize the ORN projections to the antennal lobes and mouse nc82 (DSHB, 1:50) was added to visualize the structure of the brain. *Pupal Antennae. Orco>mCD8::GFP* larvae were collected in 2 trays, each of which contained ~60 larvae. At the given timepoint After Puparium Formation (APF), the cephalothorax and abdomen of the pupae were extracted and the antennae, oculus, compound eye, and rudimentary appendages were placed in 4% paraformaldehyde (PFA) with 0.1% Triton Phosphate Buffer Solution (PBS-T). Antennae were then dissected out and washed 3x in 1X PBS-T (0.1%). Antennae were then blocked for 30min at 4°C with 5% Normal Goat Serum (NGS).

To visualize mCD8::GFP expression, we added rat anti-CD8 (Invitrogen #MCD0800, 1:100), which was left to incubate on a rotator overnight at 4°C. The next day, antennae were washed 3x in 1X PBS-T (0.1%) and Alexa-488 goat anti-rat (Invitrogen A110066, 1:200) was added to the solution. After 1.5hr at 25°C, antennae were washed 2X in 1X PBS-T (0.1%) and the last wash in 1xPBS to remove the triton.

Antennae were placed on slides and mounted in Slow Fade Gold medium (ThermoFisher Scientific #S36936).

Confocal imaging and analyses. Brains and pupal antennae were imaged on an LSM 700 Zeiss confocal microscope at 512x512 pixel resolution, with 0.96 or 2.37uM Z-steps. For illustration purposes, confocal images were processed using Fiji (52) to collapse the maximum intensity projection of Z-stacks into a single image. We used cells that were immunoreactive to mCD8 as a proxy for ORCO expression. Cells were counted manually.

Host-proximity assay. The design and methods of the host-proximity assay are modified from DeGennaro et al. 2013 (4). Briefly, for each trial, 20-30 adult female *Anopheles* mosquitoes (5+ days post eclosion, mated but not blood-fed) were sorted under cold anesthesia (4°C), placed in 24-oz deli containers (https://www.amazon.com/gp/product/B00NB9WCEO/ref=oh_aui_detailpage_o06_s00?ie=UTF8&psc=1), and fasted with access to water for 16-24hr prior to assaying. Pre-fasting and behavior experiments took place at 27°C and 70-80% relative humidity. Experiments took placed after Zeitgeber Time 0 (ZT0) and continued until ZT8. 5 minutes before the start of the assay, mosquitoes were released into a modified BugDorm (https://shop.bugdorm.com/bugdorm-1-insect-rearing-cage-p-1.html). After 5 minutes had elapsed, pure CO_2 and synthetic air (air flow rate: 0.1L/min, CO_2 flowrate 145MM) were mixed in an adaptor before being pulsed (3sec on: 3 sec off) into a flypad (8.1 x 11.6cml catalogue #59-114; Flystuff.com, San Diego, CA), which was placed at

the bottom of the BugDorm. Mosquitoes were then presented with a single volunteer's arm, which was placed 2.5cm away from one side of the BugDorm so that mosquitoes could not come into direct contact with the arm. To control the distance from the arm to the cage, a Q-Snap needlework frame (https://www.amazon.com/dp/B00013MV30/ref=twister_B07CQQJKL2?_encoding=UTF8&psc=1) was placed flush against the cage and the arm was pressed against the vials. The arm was elevated 2.7cm by placing it on a plastic microcentrifuge test-tube rack. An HDR-CX260V camera (Sony) was positioned to take images of mosquitoes responding to the human arm. Trials ran for 3 minutes. To quantify mosquito responses that came into 'close proximity' to the human arm, we counted the number of mosquitoes resting on the screen. We did not include mosquitoes that had landed on the white area surrounding the screen nor the mosquitoes that were in flight. For the % attraction figure, we scored the number of mosquitoes that came into close proximity of the arm every 10 seconds from minute 1 to minute 3 and then divided this number by the total number of mosquitoes in the trial. Data were analyzed using JMP Version 9, SAS Institute Inc., Cary, NC, 1989-2019.

Author Contributions: S.E.M and C.J.P. designed research; S.E.M., A.A., and L.A.G. performed research; S.E.M. and L.A.G. analyzed data; and S.E.M. and C.J.P. wrote the paper.

Acknowledgments: This research benefited from the limitless enthusiasm and support of Potter Lab members, both past and present. In particular, we would like to thank

Kateline Robinson Shaw and Liz Marr for assisting with molecular biology. Darya Task and Joanna Konopka helped rear the transgenic mosquitoes and improved the writing of the manuscript. We also thank Greg Artiushin for the graphic designs he made for the paper. This work was supported by grants from the National Institutes of Health to C.J.P. (NIAID R01AI137078), the Department of Defense to C.J.P. (W81XWH-17-PRMRP), and a Johns Hopkins Malaria Research Institute Postdoctoral Fellowship to SEM. We thank the Johns Hopkins Malaria Research Institute and Bloomberg Philanthropies for their support.

REFERENCES

1. Global Malaria Programme WG (2019) World malaria report 2019. ed WHO, p 232.

2. Cowman A, Healer J, Marapana D, & Marsh K (2016) Malaria: biology and disease. Cell 167(3):610-624.

3. Beauty B & Marquardt W (1996) The Biology of Disease Vectors (University Press of Colorado) 1 Ed.

4. DeGennaro M, et al. (2013) orco mutant mosquitoes lose strong preference for humans and are not repelled by volatile DEET. Nature 498(7455):487-491.

5. Butterwick J, et al. (2018) Cryo-EM structure of the insect olfactory receptor Orco. Nature 560.

6. Riabinina O, et al. (2016) Organization of olfactory centers in the malaria mosquito *Anopheles gambiae*. Nature Communications 7(13010).

7. VectorBase (Giraldo-Calderón et al 2015), *Anopheles gambiae* PEST, AgamP4.12.

671 8. Couto A, Alenius M, & Dickson B (2005) Molecular, Anatomical, and Functional
672 Organization of the *Drosophila* Olfactory System. Current Biology 15(17):1535-1547.
673 9. Ghaninia M, Hansson B, & Ignell R (2007) The antennal lobe of the African malaria
674 mosquito, *Anopheles gambiae* - innervation and three-dimensional reconstruction.
675 Arthropod Structure & Development 36(1):23-39.
676 10. Bell J & Wilson R (2016) Behavior reveals selective summation and max pooling
677 among olfactory processing channels. Neuron 91(2):425-438.
678 11. Clark J & Ray A (2016) Olfactory mechanisms for discovery of odorants to reduce
679 insect-host contact. Journal of Chemical Ecology 42:919-930.
680 12. Jones P, Pask G, Rinker D, & Zwiebel L (2011) Functional agonism of insect
681 odorant receptor ion channels. Proceedings of the National Academy of Science USA
682 108(21):8821-8825.
683 13. Carey A & Carlson J (2011) Insect olfaction from model systems to disease control.
684 Proceedings of the National Academy of Science USA 108(32):12987-12995.
685 14. Chin S, Maguire S, Huoviala P, Jefferis G, & Potter C (2018) Olfactory neurons and
686 brain centers directing oviposition decisions in *Drosophila.* Cell Reports 24(6):1667-
687 1678.
688 15. Riabinina O, et al. (2015) Improved and expanded Q-system reagents for genetic
689 manipulations. Nature Methods 12(3):219-222.
690 16. Carey A, Wang G, Su C-Y, Zwiebel L, & Carlson J (2010) Odorant reception in the
691 malaria mosquito *Anopheles gambiae*. Nature 464(7285):66-71.
692 17. Potter C & Luo L (2010) Splinkerette PCR for mapping transposable elements in
693 *Drosophila*. PloS One 5(4):e10168.

694 18. Dobritsa A, van der Goes van Naters W, Warr C, Steinbrecht A, & Carlson J (2003)
695 Integrating the molecular and cellular basis of odor coding in the *Drosophila* antenna.
696 Neuron 37(5):827-841.
697 19. Hallem E, Ho M, & Carlson J (2004) The molecular basis of odor coding in the
698 *Drosophila* antenna. Cell 117(7):965-979.
699 20. Ray A, van der Goes van Naters W, Shiraiwa T, & Carlson J (2007) Mechanisms of
700 odor receptor gene choice in *Drosophila*. Neuron 53:353-369.
701 21. Mysore K, Flister S, Müller P, Rodrigues V, & Reichert H (2011) Brain development
702 in the yellow fever mosquito *Aedes aegypti*: a comparative immunocytochemical
703 analysis using cross-reacting antibodies from *Drosophila melanogaster*. Developmental
704 Genes and Evolution 221:281-296.
705 22. Mysore K, Flannery E, Tomchaney M, Severson D, & Duman-Scheel M (2013)
706 Disruption of *Aedes aegypti* olfactory system development through Chitosan/siRNA
707 nanoparticle targeting of semaphorin-1a. PloS Neglected Tropical Diseases 7(5):e2215.
708 23. Mysore K, Andrews E, Li P, & Duman-Scheel (2014) Chitosan/siRNA nanoparticle
709 targeting demonstrates a requirement for single-minded during larval and pupal
710 olfactory system development of the vector mosquito *Aedes aegypti*. BMC
711 Developmental Biology 14(9).
712 24. Raji J, et al. (2019) *Aedes aegypti* mosquitoes detect acidic volatiles found in human
713 odor using the IR8a pathway. Current Biology 29:1253-1262.
714 25. Serizawa S, et al. (2003) Negative feedback regulation ensures the one receptor-
715 one olfactory neuron rule in mouse. Science 302(5653):2088-2094.

716 26. Feinstein P, Bozza T, Rodriguez I, Vassalli A, & Mombaerts P (2004) Axon
717 guidance of mouse olfactory sensory neurons by odorant receptors and the β2
718 adrenergic receptor. Cell 117.
719 27. Lewcock J & Reed R (2004) A feedback mechanism regulates monoallelic odorant
720 receptor expression. Proceedings of the National Academy of Science USA
721 101(4):1069-1074.
722 28. Shykind B, et al. (2004) Gene switching and the stability of odorant receptor gene
723 choice. Cell 117(6):801-815.
724 29. Dalton R, Lyons D, & Lomvardas S (2013) Co-opting the unfolded protein response
725 to elicit olfactory receptor feedback. Cell 155:321-332.
726 30. Vassar R, et al. (1994) Topographic organization of sensory projections to the
727 olfactory bulb. Cell 79.
728 31. Mombaerts P, et al. (1996) Visualizing an olfactory sensory map. Cell 87:675-686.
729 32. Wang F, Nemes A, Mendelsohn M, & Axel R (1998) Odorant receptors govern the
730 formation of a precise topographic map. Cell 93:47-60.
731 33. Clowney E, et al. (2012) Nuclear aggregation of olfactory receptor genes governs
732 their monogenic expression. Cell 151(4):724-737.
733 34. Omondi A, Ghaninia M, Dawit M, Svensson T, & Ignell R (2019) Age-dependent
734 regulation of host seeking in *Anopheles coluzzii*. Scientific Reports 9(9699).
735 35. Foster W & Takken W (2004) Nectar-related vs. human-related volatiles:
736 behavioural response and choice by female and male *Anopheles gambiae*
737 (Diptera:Culicidae) between emergence and first feeding. Bulletin of Entomological
738 Research 94:145-157.

739 36. Tallon A, Hill S, & Ignell R (2019) Sex and age modulate antennal chemosensory-
740 related genes linked to the onset of host seeking in the yellow-fever mosquito, *Aedes*
741 *aegypti*. Scientific Reports 9(43).
742 37. Nguyen M, Zhou Z, Marks C, Ryba N, & Belluscio L (2007) Prominent roles for
743 odorant receptor coding sequences in allelic exclusion. Cell 131(5):1009-1017.
744 38. Karner T, Kellner I, Schultze A, Breer H, & Krieger J (2015) Co-expression of six
745 tightly clustered odorant receptor genes in the antenna of the malaria mosquito
746 *Anopheles gambiae*. Frontiers in Ecology and Evolution 3(26).
747 39. Hill C, et al. (2002) G protein-coupled receptors in *Anopheles gambiae*. Science
748 298.
749 40. Bohbot J, et al. (2007) Molecular characterization of the *Aedes aegypti* odorant
750 receptor gene family. Insect Molecular Biology 16(5):525-537.
751 41. Zhang X, Rodriguez I, Mombaerts P, & Firestein S (2004) Odorant and vomeronasal
752 receptor genes in two mouse genome assemblies. Genomics 83:802-811.
753 42. Sullivan S, Adamson M, Ressler K, Kozak C, & Buck L (1996) The chromosomal
754 distribution of mouse odorant receptor genes. Proceedings of the National Academy of
755 Science USA 93:884-888.
756 43. Benton R, Sachse S, Michnick S, & Vosshall L (2006) Atypical membrane topology
757 and heteromeric function of *Drosophila* odorant receptors in vivo. PloS Biology 4(2):e20.
758 44. German P, van der Poel S, Carraher C, Kralicek A, & Newcomb R (2013) Insights
759 into subunit interactions within the insect olfactory receptor complex using FRET. Insect
760 Biochemistry and Molecular Biology 43(2):138-145.

761 45. Neuhaus E, et al. (2005) Odorant receptor heterodimerization in the olfactory
762 system of *Drosophila melanogaster*. Nature Neuroscience 8(1):15-17.
763 46. Tsitoura P, et al. (2010) Expression and membrane topology of *Anopheles gambiae*
764 odorant receptors in Lepidopteran Insect Cells. PloS One 5(11):e15428.
765 47. Athrey G, Cosme L, Popkin-Hall Z, Pathikonda W, & Slotman M (2017)
766 Chemosensory gene expression in olfactory organs of the anthropophilic *Anopheles*
767 *coluzzii* and zoophilic *Anopheles quadriannulatus*. BMC Genomics 18(1):751.
768 48. Pitts R, Rinker D, Jones P, Rokas A, & Zwiebel L (2011) Transcriptome profiling of
769 chemosensory appendages in the malaria vector *Anopheles gambiae* reveals tissue-
770 and sex-specific signatures of odor coding. BMC Genomics 12(271).
771 49. McMeniman C, Corfas R, Matthews B, Ritchie S, & Vosshall L (2014) Multimodal
772 integration of carbon dioxide and other sensory cues drives mosquito attraction to
773 humans. Cell 156:1060-1071.
774 50. Greppi C, et al. (2020) Mosquito heat seeking is driven by an ancestral cooling
775 receptor. Science 367:681-684.
776 51. Afify A, Betz J, Riabinina O, Lahondère C, & Potter C (2019) Commonly used insect
777 repellents hide human odors from *Anopheles* mosquitoes. Current Biology 29(21).
778 52. Schindelin J, et al. (2012) Fiji: an open-source platform for biological-image
779 analysis. Nature Methods 9:676-682.
780 53. Lin C-C & Potter C (2015) Re-classifcation of *Drosophila melanogaster* trichoid and
781 intermediate sensilla using fluorescence-guided single sensillum recording. PloS One.
782 54. Bray N, Pimentel H, Melsted P, & Pachter L (2016) Near-optimal probabilistic RNA-
783 seq quantification. Nature Biotechnology 34(5).

784 55. Pimentel H, Bray N, Puente S, Melsted P, & Pachter L (2017) Differential analysis of
785 RNA-Seq incorporating quantification uncertainty. Nature Methods 14:687-690.
786 56. Hamilton N & Ferry M (2018) ggtern: Ternary Diagrams Using ggplot2. Journal of
787 Statistical Software, Code Snippets 87(3):1-17.

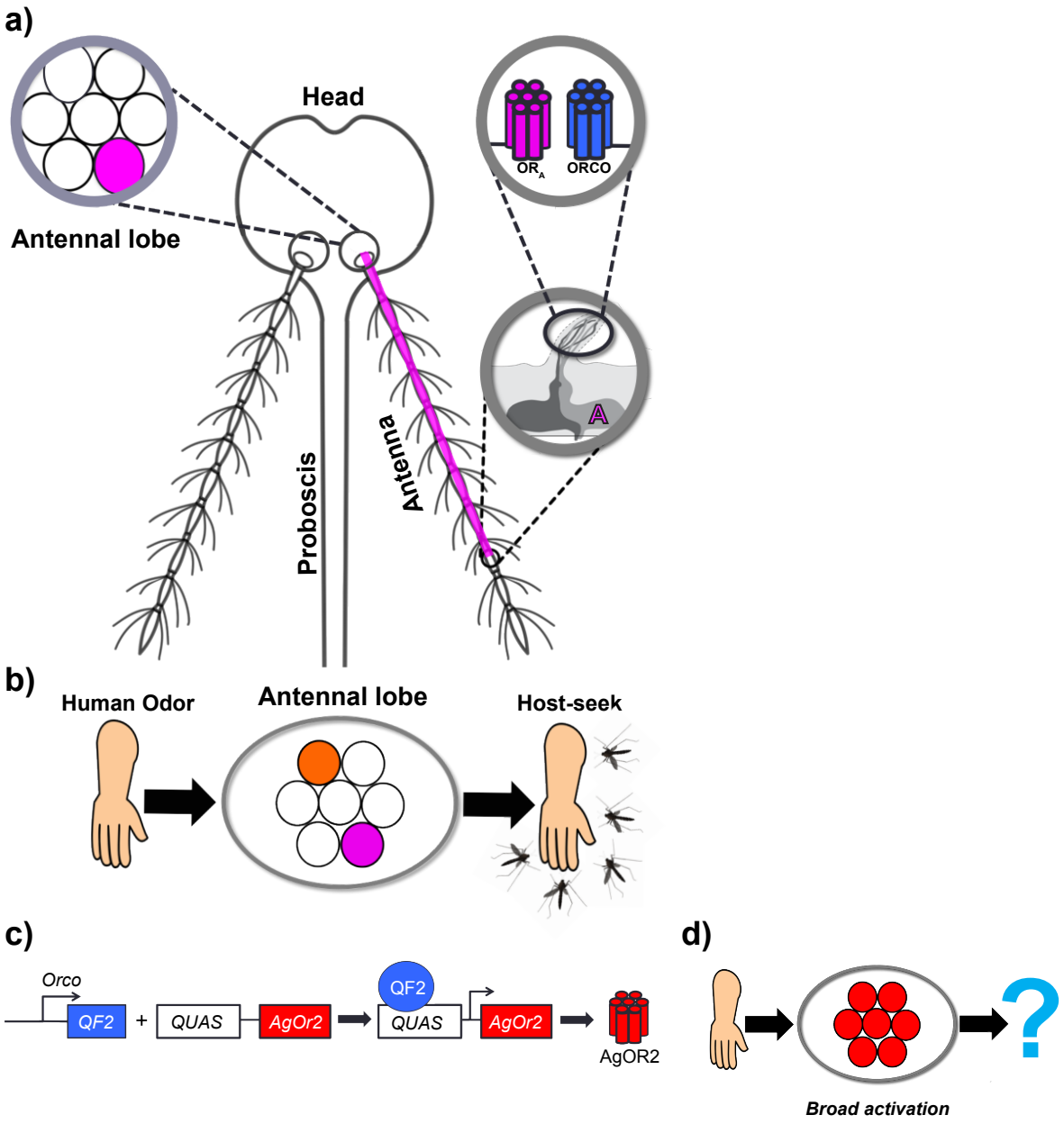

788 **Figure 1. Strategy to manipulate the olfactory system of *Anopheles* mosquitoes.**
789 **a) Anatomy of odorant receptor guided olfaction.** Mosquitoes smell odors in the
790 environment using three olfactory organs: the proboscis, the maxillary palps (not
791 shown), and the antennae. A single antenna is made up of 13 segments called
792 'flagellomeres.' Each flagellomere is covered with sensory hairs called 'sensilla,' a

single one of which houses up to 4 olfactory neurons. An olfactory neuron expresses 1 of 3 chemosensory gene families: the *ionotropic receptors*, the *gustatory receptors,* or the *odorant receptors*. The *odorant receptor* gene family plays an important role in host-seeking behavior. There are 75 different ORs in the *Anopheles gambiae* genome, each of which is sensitive to specific odors in the environment. Only 1 OR (OR_A) is expressed *per* olfactory receptor neuron (ORN, labeled 'A'). At the dendrites of ORN A, OR_A couples with the obligate co-receptor, ORCO. When odor binds to OR_A-ORCO complexes, ORN A becomes active and sends its excitatory signal down its axon, targeting a discrete brain region of the mosquito antennae lobe (AL) called a 'glomerulus' (shown as a pink circle). **b) A human-specific odor code in the mosquito brain.** Human odors bind to specific ORs, activating the ORNs on which they are expressed. Activated ORNs target discrete glomeruli (pink, orange) in the AL to guide host-seeking. **c) Olfactogenetics strategy.** Using the Q-system, the *Orco-QF2* transgene (6) was combined with the effector construct, *QUAS-AgOr2*. The combination of these transgenes causes AgOR2 to be expressed in *Orco*-positive ORNs. **d) Test of the olfactogenetics strategy.** AgOR2 responds to major components of human odor such as indole and benzaldehyde. We hypothesized that *Orco>AgOr2* mosquitoes would experience broad activation of the majority of the AL in the presence a human, thereby dysregulating the human-specific odor code in the mosquito brain (**Fig. 1b**). *Orco>AgOr2* mosquitoes would then be evaluated on whether they showed reduced host-seeking behavior.

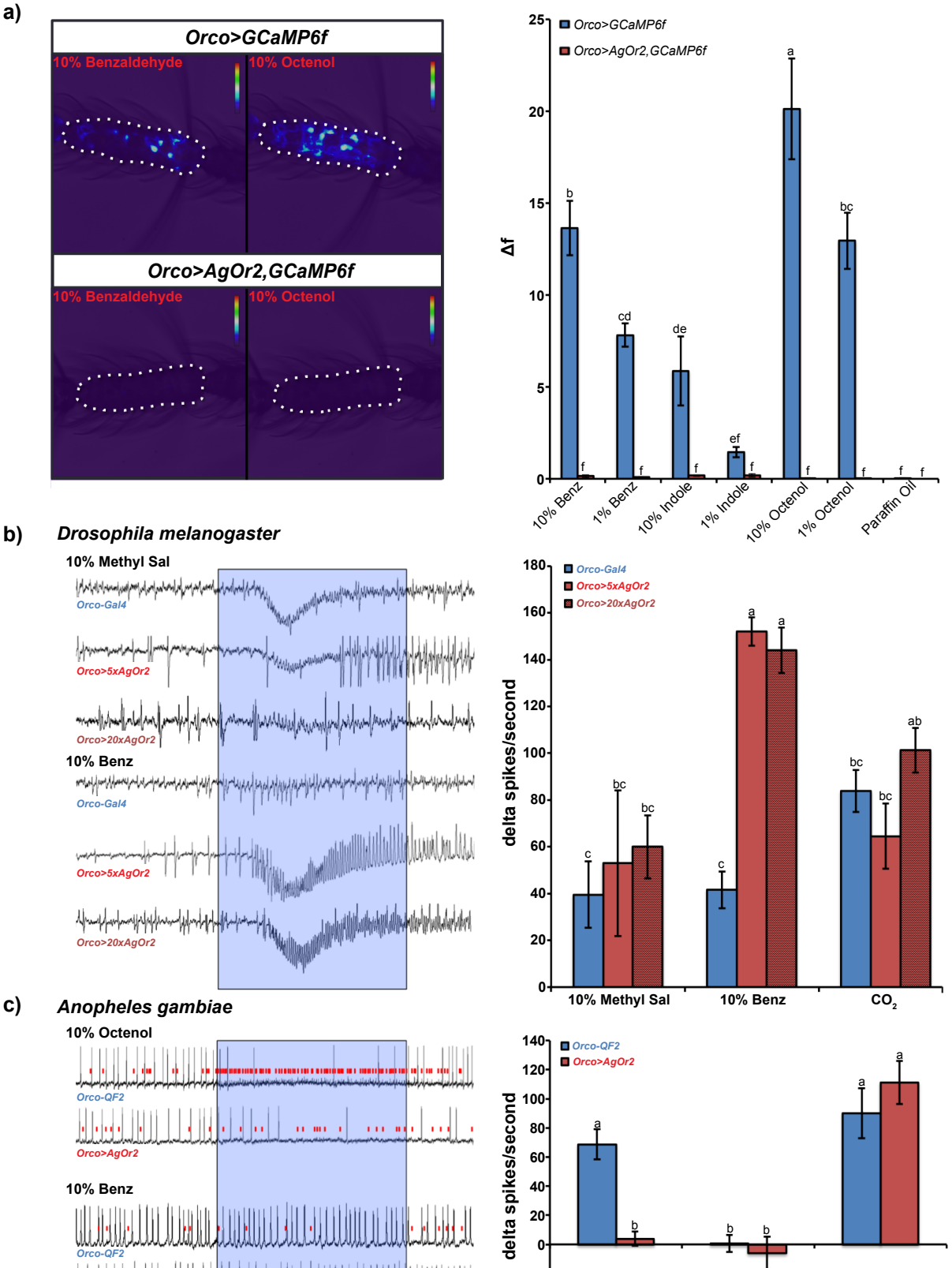

Figure 2. Olfactogenetics impairs *Anopheles* but not *Drosophila Orco*-positive ORNs. a) *Orco>AgOr2,GCamp6f* mosquitoes show impaired olfactory responses to human odorants. The activity of olfactory receptor neurons in antennal segment 11 (outlined with a white dotted line) was detected by calcium imaging of *Orco*-positive neurons expressing *GCaMP6f* (51). Relative to controls (*Orco>GCaMP6f)*, mosquito antennal segments with ectopic expression of *AgOr2* and *GCaMP6f* (*Orco>AgOr2,GCaMP6f)* show impaired responses to benzaldehyde (10% and 1%) and indole (10%), the cognate ligands of AgOR2. They also show dampened responses to octenol (10% and 1%). A two-way repeated measures ANOVA was conducted to test the effect of odor and genotype on calcium responses. We found a significant effect at the $p<0.0001$ level. Groups with different letter values (a-f) are statistically different as determined by the Tukey post hoc HSD test. Each sample included in the analysis was taken from a different female mosquito. $n_{Orco>GCaMP6f} = 9$, $n_{Orco>AgOr2,GCaMP6f} = 8$. **b) Ectopic expression of *AgOr2* in *Drosophila* ab1 sensilla does not impair ORN physiology.** The cognate ligand of OR10a-expressing neurons is methyl salicylate (Methyl Sal). Driving *AgOr2* into this neuronal group using the *5xUAS* or *20xUAS* effector lines does not affect OR10a's response to Methyl Sal. *Orco*-positive ORNs of *Orco>5xAgOr2* and *Orco>20xAgOr2* animals show an ectopic response to benzaldehyde (Benz). The presence of the *Orco*-negative CO_2 neuron was used to verify that recordings were taken from the ab1 sensillum. The activity of the CO_2 neuron (trace not shown) is not affected by the experimental manipulation. Odor or CO_2 stimulus was delivered in the timeframe denoted by the blue translucent box. A two-way repeated measures ANOVA was used to determine significance of genotype and odor

837 on delta spikes/second at the *p<0.0001* level. Groups with different letter values (a-c)
838 are statistically different as determined by the Tukey post hoc HSD test. 2-3 Females
839 *per* genotype were analyzed. The number of sensilla evaluated for each group: $n_{Orco\text{-}GAL4}$ = 9; $n_{Orco>5xAgOr2}$ = 4; $n_{Orco>20xAgOr2}$ = 5. **c) Olfactogenetics impairs *Orco*-positive**
841 **ORN physiology in *Anopheles.*** Single sensillum recordings from the *Anopheles*
842 maxillary palp capitate peg sensilla. The cognate ligand of OR8-expressing neurons is
843 octenol. Driving *AgOr2* into this neuron group interferes with OR8's response to octenol
844 (smallest spiking neurons, red lines indicate OR8 activity). The ORNs ectopically
845 expressing *AgOr2* do not respond to benzaldehyde (Benz). The presence of the *Orco*-
846 negative CO_2 neuron was used to verify that recordings were taken from a cp sensillum.
847 The activity of the CO_2 neuron (trace not shown) was not affected by the experimental
848 manipulation. Odor or CO_2 was delivered in the timeframe denoted by the blue
849 translucent box. A two-way repeated measures ANOVA was used to determine that
850 there was a significant effect at the $p<0.005$ level of odor and genotype on delta
851 spikes/second. Groups with different letter values (a-b) are statistically different as
852 determined by the Tukey post doc HSD test. 2-3 Females *per* genotype were analyzed.
853 The number of sensilla evaluated for each group: $n_{Orco\text{-}QF2}$ = 6; $n_{Orco>AgOr2}$ = 5. Error bars
854 represent the standard error (SEM).

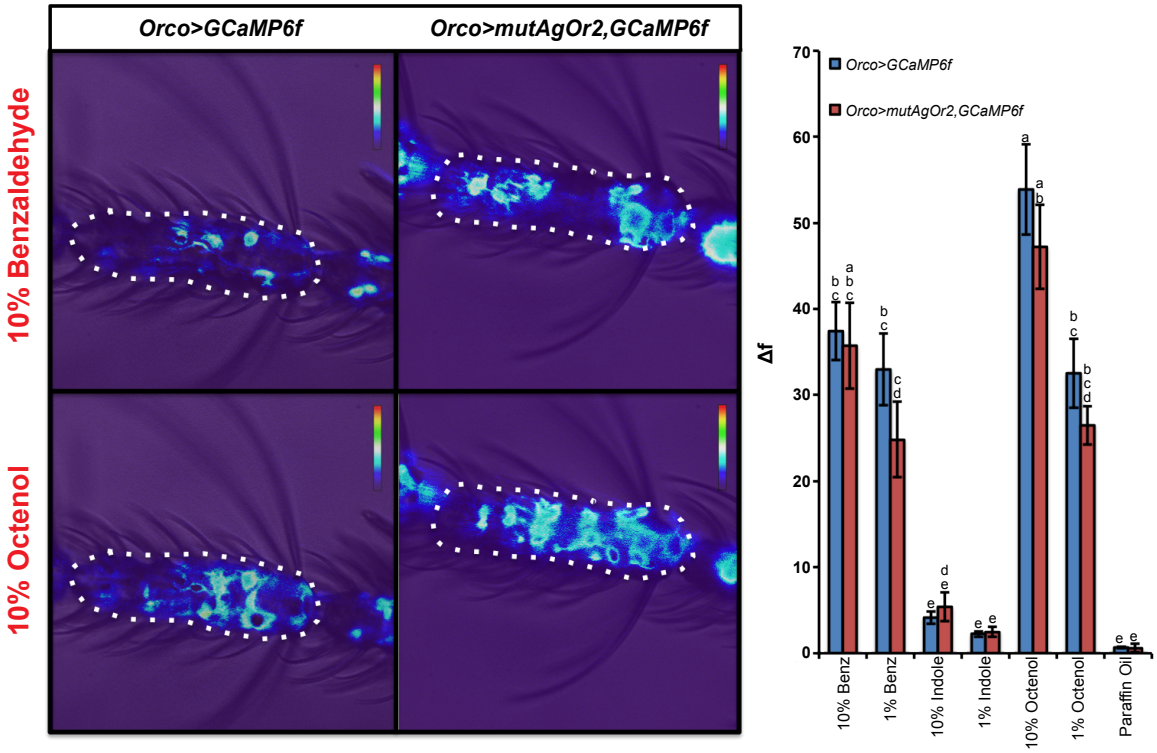

855 **Figure 3. AgOR2 protein is required for the dominant negative olfactory**
856 **phenotype caused by *Orco>AgOr2* expression.** The *mutAgOR2* transgene contains
857 an introduced point mutation in the start codon of *AgOr2* and a frameshift mutation at a
858 second in-frame ATG site of the gene. Odor-evoked responses (Δf) were calculated
859 from the 11th segment of the mosquito antennae (outlined by dotted lines).
860 Representative control and experimental calcium imaging responses to 10%
861 benzaldehyde and 10% octenol are shown. Antennae from *Orco>mutAgOr2,GCaMP6f*
862 mosquitoes show no difference in responses to odors from control (*Orco>GCaMP6f*). A
863 two-way repeated measures ANOVA was used to determine that there was a significant
864 effect at the $p<0.005$ level of odor and genotype on calcium responses. Groups with
865 different letter values (a-d) are statistically different as determined by the Tukey post
866 hoc HSD test. Error bars represent the standard error (SEM). Each sample included in

867 the analysis was taken from a different female mosquito. $n_{Orco>GCaMP6f}$ = 11,

868 $n_{Orco>mutAgOr2,GCaMP6f}$ = 5.

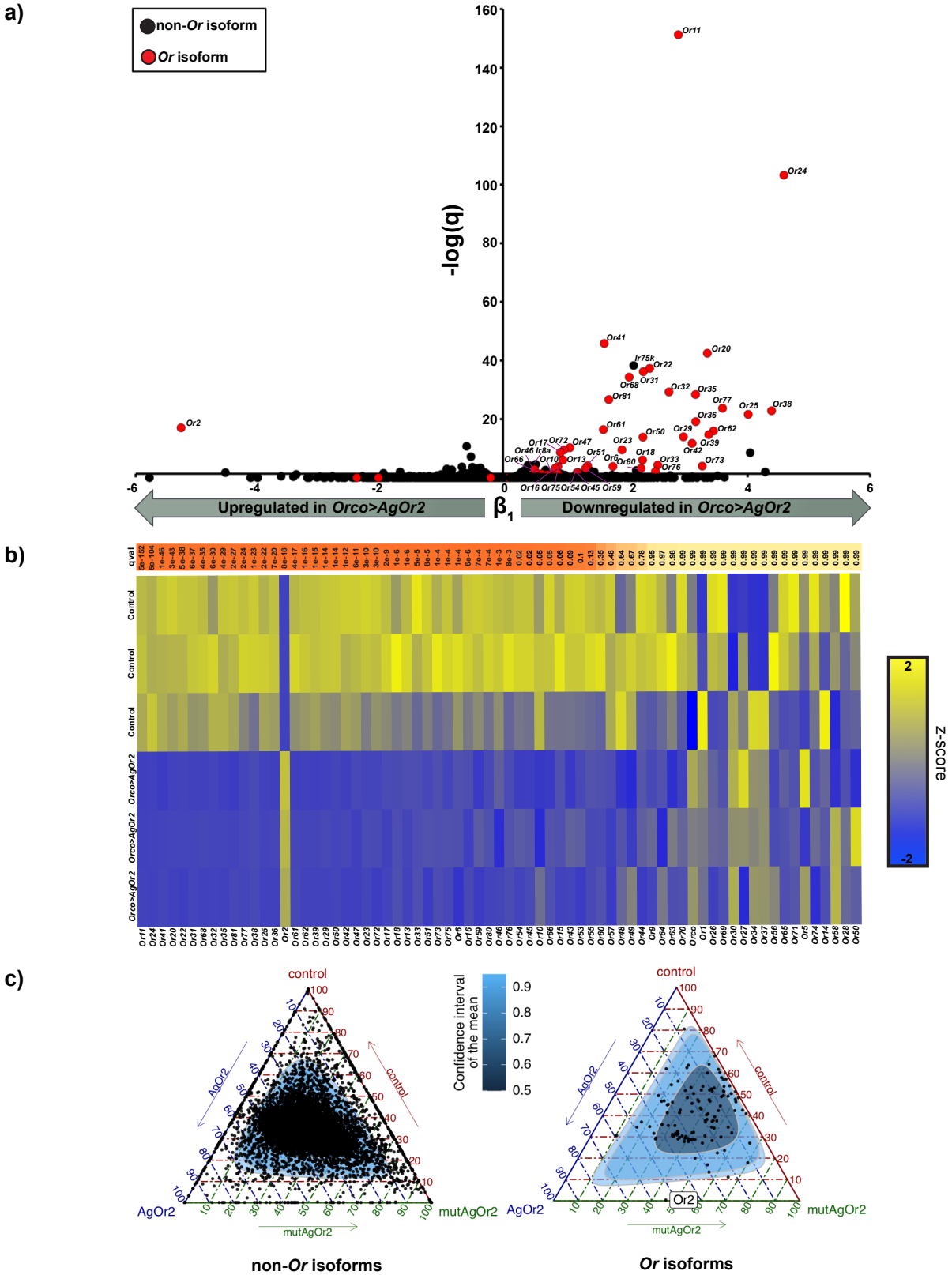

Figure 4. Ectopic AgOR2 protein reduces the transcript levels of *Or* isoforms. a) Volcano plot of differentially expressed isoforms. Using Wald tests, we evaluated whether the 13224 isoforms present in 3 triplicates of control and 3 triplicates of *Orco>AgOr2* antennae (~200 antennae *per* sample) were differentially expressed. *Non-odorant receptor* and *odorant receptor* isoforms are shown as black or red dots, respectively. Only 0.63% of the transcriptome is differentially regulated in *Orco>AgOr2,* where 49% of those transcripts are *Ors.* –log(q) is the level of significance of β_1, which, for each isoform, is defined as $TPM_{control}$ -$TPM_{experimental}$. The 41 *Ors* found significant from the Wald tests are labeled according to their gene annotation in the volcano plot. All *Ors* (with the exception of *AgOr2*) that are differentially expressed are downregulated in the experimental condition. Interestingly, *Ir8a* and *Ir75k* (indicated on the volcano plot) are downregulated in *Orco>AgOr2*. The remaining *Irs* and *Grs* are unaffected. **b) Heatmap of the *Or* gene family.** A z-score was computed for each cell in the heatmap by subtracting the mean isoform TPM from the cell's TPM divided by the standard deviation of the isoform TPM. *Ors* are sorted along the X-axis according to their significance level (q value) from the Wald tests in **a**. Darker orange is most significant, yellow is not significant. *Ors* are downregulated in *Orco>AgOr2* samples, with the exception of *AgOr2,* which is upregulated. **c) Ectopic AgOR2 protein is required for the observed downregulation of native *Or* transcripts.** Ternary plots were used to visualize the relative ratio of a genotype to an isoform's relative abundance level using the formula: $(TPM_{genotypeX})/(\text{mean } TPM_{control} + \text{mean } TPM_{Orco>AgOr2} + \text{mean } TPM_{Orco>mutAgOr2})*100$. (left) There are equal ratios of transcript abundance levels for non-*Or* genes among the three genotypes (right). However, the relative contribution to

892 transcript abundance levels of control, *Orco>AgOr2,* and *Orco>mutAgOr2* are skewed
893 in the *Or* gene family such that *Or* gene levels in *Orco>mutAgOr2* and control are
894 relatively similar and higher than *Orco>AgOr2* levels, with the exception of *AgOr2* itself
895 (whose abundance is similar between *Orco>AgOr2* and *Orco>mutAgOr2*).

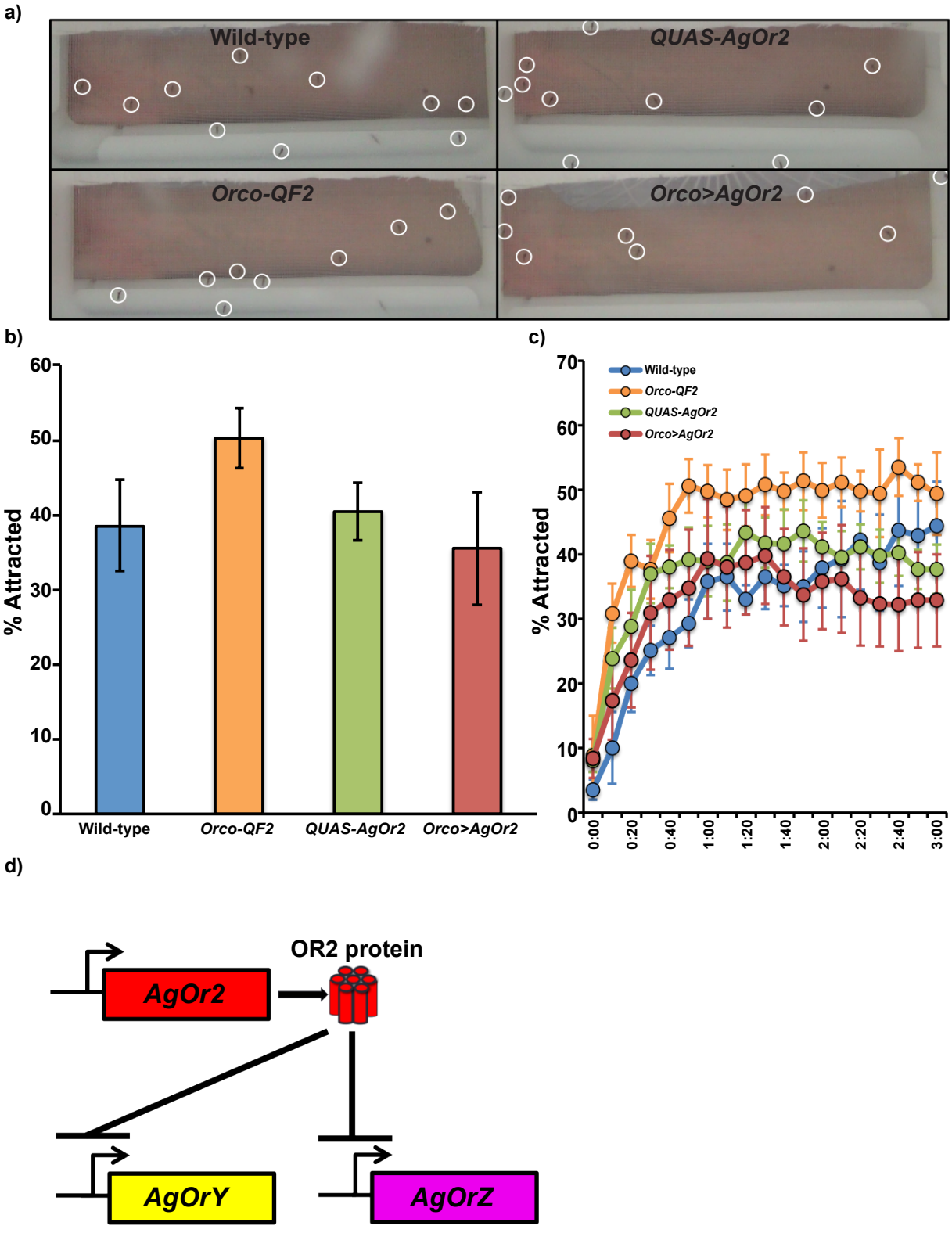

896 **Figure 5. *Orco>AgOr2* mosquitoes remain attracted to a human host. a)**

897 Representative images of wild-type, *Orco-QF2*, *QUAS-AgOr2*, and *Orco>AgOr2*

mosquitoes (circled) in the host-proximity assay. Mosquitoes attracted to an arm (2.5cm from the cage) that land on the net are counted. **b) Results of the host-proximity assay.** A one-way ANOVA between subjects was conducted to compare the effect of genotype on % attraction. There was no effect of genotype on % attraction at the $p<0.05$ level for the four groups ($F(3)$ = 1.08, p=.37). Error bars represent the standard error (SEM). 20-30 female mosquitoes were tested *per* trial. The number of trials *per* genotype: $n_{\text{Wild-type}}$ = 5; $n_{Orco\text{-}QF2}$ = 5; $n_{QUAS\text{-}AgOr2}$ = 7; $n_{Orco>AgOr2}$ = 7 **c) Time course of mosquito attraction towards a human host by genotype**. Over the course of 3 minutes, there was no difference in the % of mosquitoes attracted to a human host. **d) Summary Model: ectopic AgOR2 negatively regulates the expression of *Or* transcripts.** Our data implicates a mechanism of negative regulation of most *Or* transcripts (for example, *OrY* and *OrZ*) by ectopic AgOR2 protein.

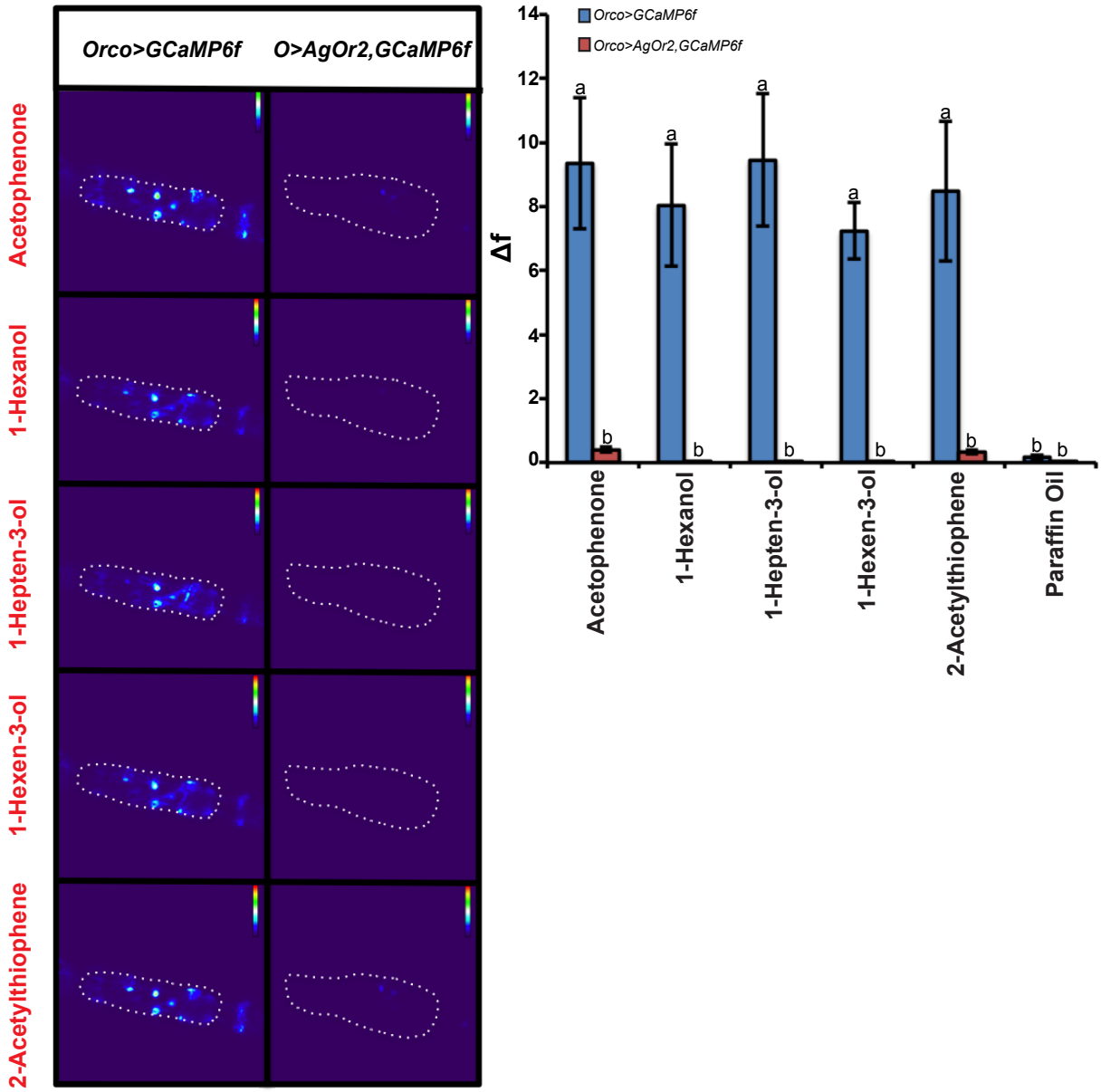

910 **Supplementary Figure 1. Antennae with ectopic *AgOr2* expression fail to respond**
911 **to odors that activate multiple ORN classes.** The activity of olfactory receptor
912 neurons in antennal segment 11 (outlined by white dots) towards the listed odors were
913 detected by calcium imaging of *Orco*-positive neurons expressing GCaMP6f (51).
914 *Orco>AgOr2,GCaMP6f* is listed here as *O>AgOr2,GCaMP6f.* All odors were presented
915 at a 10% concentration. A two-way repeated measures ANOVA was used to determine

916 that there was a significant effect at the $p<0.005$ level of odor and genotype on calcium
917 responses. Groups with different letter values (a-b) are statistically different as
918 determined by the Tukey post hoc HSD test. According to Carey et al. 2010 (16),
919 acetophenone, 1-hexanol, 1-hepten-3-ol, 1-hexen-3-ol, 2-acetylthiophene activate 16,
920 14, 16, 14, 15 of the tested ORs, respectively, at a rate of $\geq$50 spikes/sec. Each sample
921 included in the analysis was taken from a different female mosquito. $n_{Orco>GCaMP6f} = 5$,
922 $n_{Orco>AgOr2,GCaMP6f} = 9$.

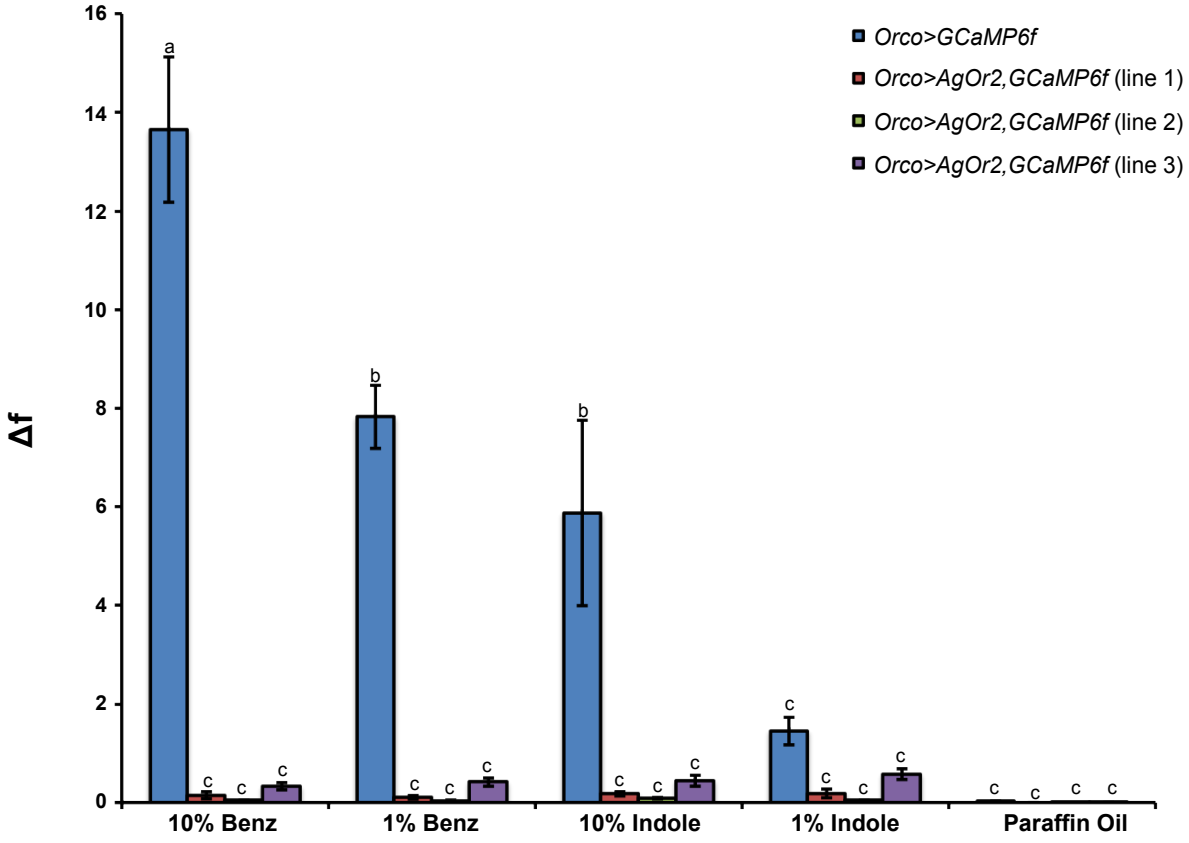

923 **Supplementary Figure 2. The dominant negative phenotype of *Orco>AgOr2* is**
924 **independent of the *QUAS-AgOr2* insertion site into the genome.** Two additional
925 *QUAS-AgOr2* lines (lines 2 and 3) show impaired physiology in the presence of
926 benzaldehyde and indole when compared to wild-type. A two-way repeated measures
927 ANOVA was used to determine that there was a significant effect of genotype and odor
928 on calcium responses at the *p<0.0001* level. Groups with different letter values (a-c) are
929 statistically different as determined by the Tukey post hoc HSD test. Each sample
930 included in the analysis was taken from a different female mosquito. $n_{Orco>GCaMP6f} = 9$;
931 $n_{Orco>AgOr2,GCaMP6f\ (line\ 1)} = 8$; $n_{Orco>AgOr2,GCaMP6f\ (line\ 2)} = 7$; $n_{Orco>AgOr2,GCaMP6f\ (line\ 3)} = 9$.

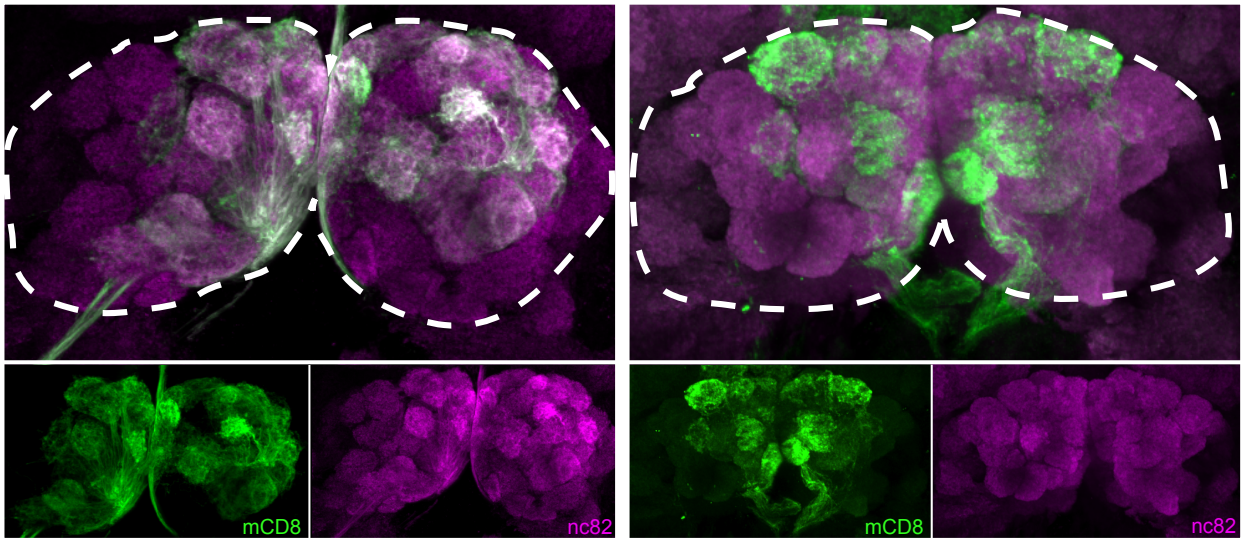

Orco>mCD8::GFP ***Orco>AgOr2,mCD8::GFP***

Supplementary Figure 3. *Orco*-positive neuron processes are present in the adult *Orco>AgOr2,mCD8::GFP* antennal lobe. *Orco*-positive ORNs send their projections to the antennal lobe of control (*Orco>mCD8::GFP*) and experimental *(Orco>AgOr2, mCD8::GFP*) lines. Anti-nc82 was used to visualize the structure of the antennal lobes and anti-CD8 was used to visualize ORN projections. Antennal lobes are outlined with white dotted lines. $n_{Orco>mCD8::GFP} = 9$; $n_{Orco>AgOr2,mCD8::GFP} = 2$.

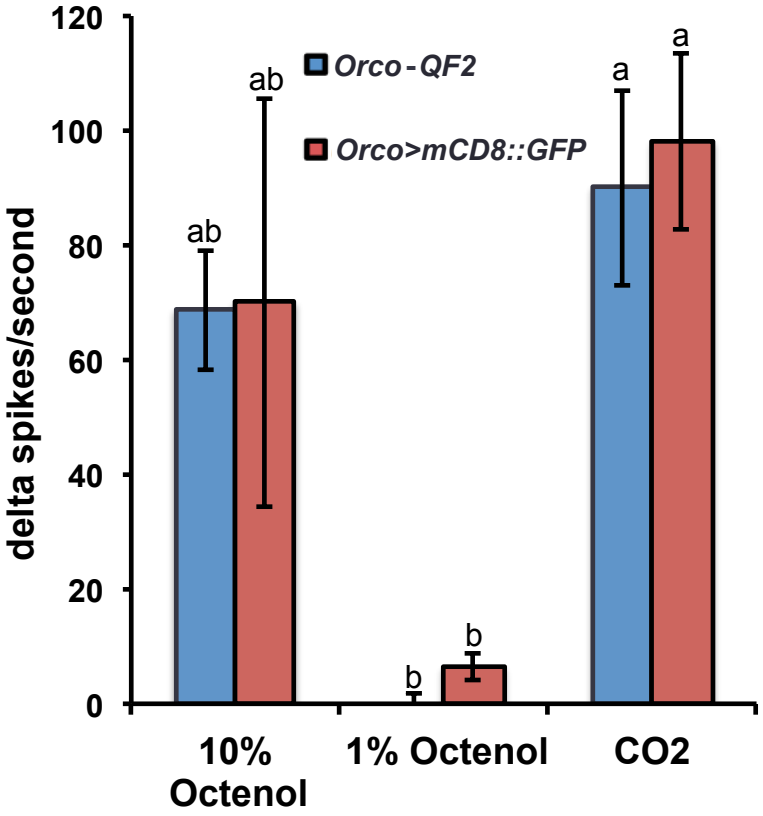

938 **Supplemental Figure 4. Driving a generic membrane-bound protein (*mCD8::GFP*)**
939 **does not impair *Orco*-positive responses to odor.** Single sensillum recordings were
940 performed in the maxillary palp capitate peg sensilla. There was no difference in how
941 cpB/C neurons of *Orco>mCD8::GFP* and *Orco-QF2* genotypes responded to 10% and
942 1% octenol. The presence of the *Orco*-negative CO_2 neuron was used to verify that we
943 were recording from a cp sensillum. A two-way repeated measures ANOVA was used to
944 determine that there was a significant effect at the $p<0.005$ level of odor but not
945 genotype on neuronal responses. Groups with different letter values (a-b) are
946 statistically different as determined by the Tukey post hoc HSD test. 2-3 Females *per*
947 genotype were analyzed. The number of sensilla evaluated for each group: $n_{Orco\text{-}QF2} = 6$;
948 $n_{Orco>mCD8::GFP} = 5$.

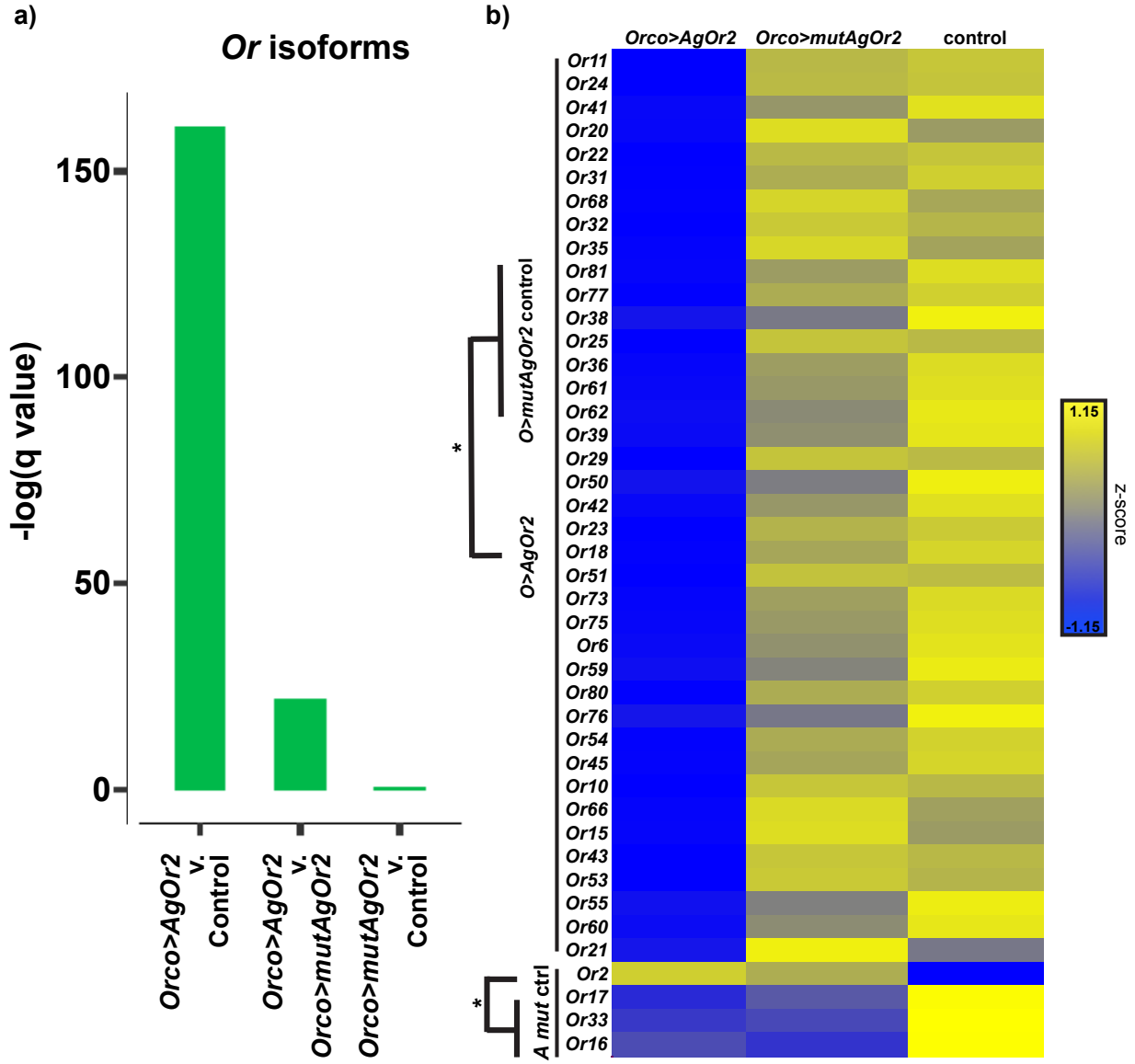

949 **Supplementary Figure 5. The majority of *Ors* are downregulated in *Orco>AgOr2***
950 **but not *Orco>mutAgOr2* and control genotypes.** Reads from 3 *Orco>AgOr2*, 3
951 *Orco>mutAgOr2*, and 5 control samples were aligned to the *Anopheles gambiae*
952 geneset AgamP4.12 (7) and samples were averaged for each group. (**a**) Results from
953 the gene set enrichment test show significant differences in *Or* isoform levels between
954 *Orco>AgOr2* v. control and *Orco>AgOr2 v. Orco>mutAgOr2.* (**b**) A heatmap was used
955 to visualize the results of pair-wise tests comparing the average isoform abundance

levels among *Orco>AgOr2, Orco>mutAgOr2,* and control groups. The first 39 *Ors* listed change between control and *Orco>AgOr2* but not control and *Orco>mutAgOr2.* The last 4 *Ors* (*Or2, Or17, Or33,* Or16) are the same between *Orco>AgOr2* (listed as '*A*') and *Orco>mutAgOr2* (listed as '*mut*') but different in control (listed as 'ctrl'). *Ors* not included in the heatmap show no differences among groups. For each cell, a z-score was calculated by subtracting the mean isoform TPM from the cell's TPM divided by the standard deviation of the isoform TPM.

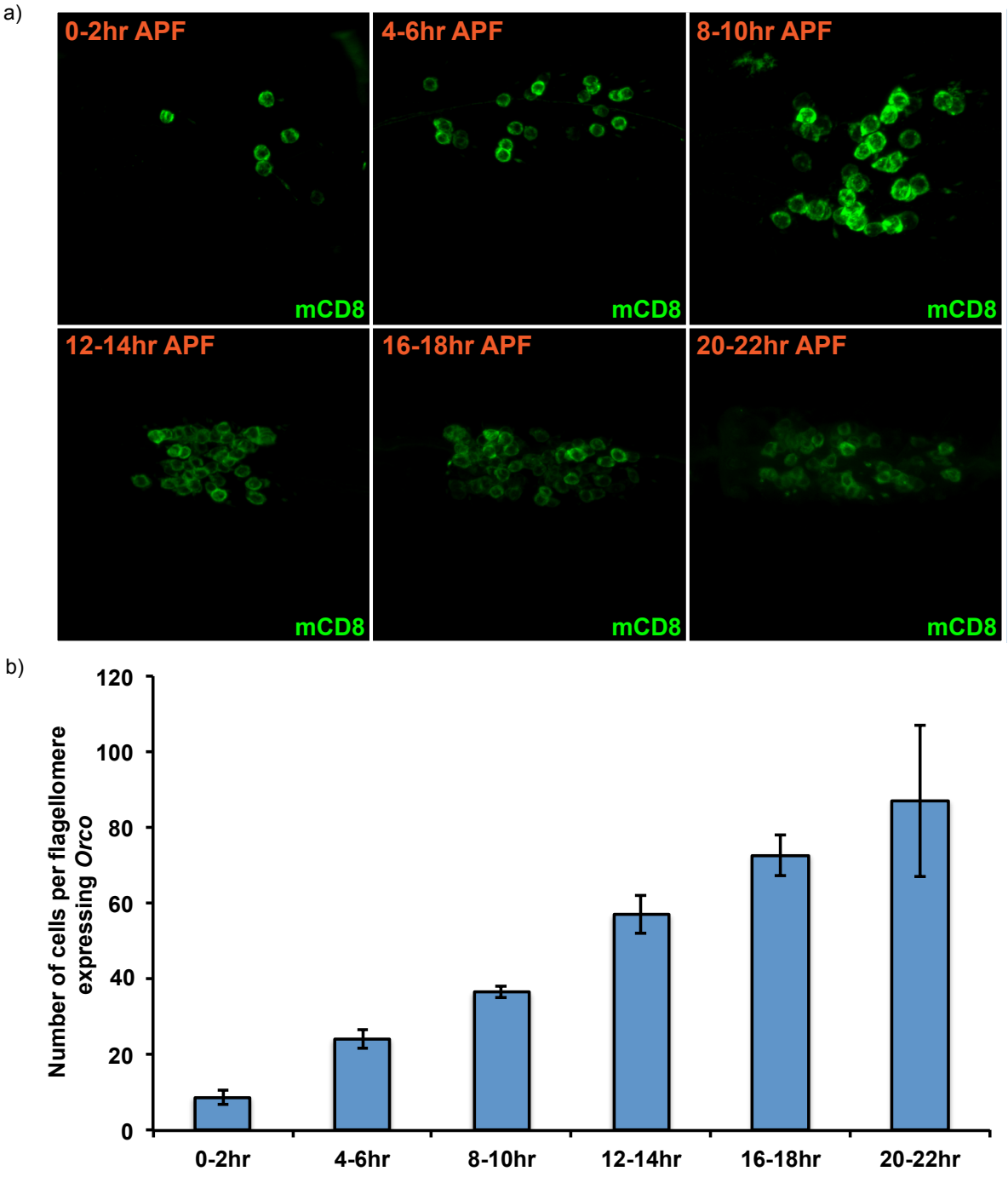

963 **Supplementary Figure 6. ORCO is expressed at the start of pupal ecdysis. a)**
964 Representative images of ORCO-expressing neurons in the *Orco>mCD8::GFP*
965 genotype. Pupal antennae were extracted at the given timepoint After Puparium
966 Formation (APF) and stained for anti-mCD8 (green). **b)** Cells were scored as ORCO-

967 positive based on the presence of mCD8. Cells from one flagellomere per animal in an
968 average of 5 animals *per* timepoint were scored. The flagellomere that was scored was
969 randomized for each sample. The error bars represent standard deviation of the mean.